Global change and global scenarios of water use and availability:
An Application of WaterGAP1.0

Joseph Alcamo, Petra Döll, Frank Kaspar and Stefan Siebert

Center for Environmental Systems Research (CESR),
University of Kassel, Germany

June, 1997

Table of contents

Summary

Although the availability of water far exceeds its use on the global scale, water resources are not evenly distributed in space or time. This report addresses the questions: What is the current distribution of global water resources? How will growth in population and economy, and changing climate affect the distribution of water in the future, and will these changes worsen or improve existing water scarcities? In this report we present some preliminary answers to these questions by using the techniques of global modeling and scenario analysis.

The WaterGAP global water model. The global scenario analysis is performed with a new global water model, WaterGAP (*Water – Global Assessment and Prognosis*) Version 1.0. WaterGAP computes water use and water availability in each of 1,162 watersheds and 160 countries covering nearly the entire terrestrial surface of the world. The model takes into account basic socio-economic factors that lead to domestic, industrial and agricultural water use, and physical and climate factors that lead to river runoff and groundwater recharge. Water "uses" in this version of the model are, specifically, water withdrawals. Water "availability" is the sum of annual river runoff and groundwater recharge. Although the model has been calibrated and tested against existing data, it nevertheless contains many limitations in its description of water use and water availability. As such, it is especially suited for drawing insights about global-scale trends, but unsuitable for detailed conclusions about individual watersheds.

Assumptions of the scenario analysis. The purpose of the scenario analysis is to estimate the influence of growth in population, economy and changing climate on future water use and availability. To do so, we investigate three scenarios of water use and two scenarios of water availability. The water use scenarios include assumptions about the trend in driving forces of water use in domestic, industrial, and agricultural sectors. They are called Scenario L(low), M (medium) or H (high) according to their level of water use. Scenario M is the "best guess" water use scenario. The *water availability* scenarios assume that surface temperature and precipitation will change in the future because of climate change. Results of the latest general circulation model of the Max-Planck-Institut are used as the "best guess" water availability scenario, while computational results of the Geophysical Fluid Dynamics Laboratory model are applied for comparison. The climate scenarios are based on the trend of greenhouse gas emissions given by the IS92a scenario of the Intergovernmental Panel on Climate Change (IPCC). Other assumptions about future developments in global population and the global economy come from the same IS92a scenario. Although WaterGAP computes changes in water use and availability for the period 1990 to 2100, in this paper we only report calculations for two "time slices" 2025 and 2075.

Indicators of criticality. Our scenario analysis focuses on the relative abundance or scarcity of water in watersheds and countries. For this purpose we use two simple indicators, the "criticality ratio" and the "criticality index". The criticality ratio (CR) is the ratio of water use to water availability in a watershed or country. The "criticality index" (CI) combines two factors – the criticality ratio and the water availability per capita – into a single indicator of water vulnerability in a watershed and country. The index ranges from 1 for water surplus to 4 for water scarcity.

The current occurrence of water scarcity. If we add up computations from all watersheds, we estimate that 30% of the world's population of 5.6 billion currently live in watersheds with water surplus (criticality index CI=1), while 20% live in marginally vulnerable watersheds (CI = 2),

6% under water stress conditions (CI = 3) and 44% in watersheds that suffer from water scarcity (CI = 4). These percentages refer to conditions in 10-percentile dry years (precipitation lower than this occurs only once every ten years). In years with average precipitation, the percentage living in watersheds with water scarcity drops to 29%.

The future occurrence of water scarcity. Under the best guess scenarios for water use (Scenario M) and water availability, we estimate that the percentage of the world's population facing water scarcity (CI = 4) increases from 44% (2.5 billion people) in 1995 to 57% (4.7 billion people) in 2025 and to 69% (7.2 billion people) in 2075. Thus, the affected population affected by water stress is predicted to double by 2025 and to triple by 2075. Under average precipitation conditions, these percentages are 29% in 1995, 37% in 2025 and 58% in 2075.

For the year 2075, the percentage of the world's population living in water scarce watersheds ranges from 61% under Scenario L to 78% under Scenario H. These data refer to dry-year conditions (the 10-percentile dry years). Water conservation measures as represented in Scenarios M and L result in a drastically improved water situation for some countries. On the other hand, most countries that have critical water scarcities (CI = 4) under Scenarios M and H remain in this category under Scenario L. In these countries it is very possible that absolute water scarcity will hinder further economic and population development. Alternatively, these countries will need to substantially increase their water availability (through desalination or inter-basin water transfers, as examples), or reduce their water demand even more radically than assumed in Scenario L.

To sum up to this point, the medium water use scenario provides a best guess of future trends, and the low and high scenarios form an uncertainty range around this guess. A robust conclusion from these three scenarios is that the intensity of current water scarcity is not likely to abate in the coming decades, and indeed may affect many more billions in the future.

The effect of climate change on the water situation. On the global average, overall annual runoff increases and water scarcity is somewhat less severe under climate change. We can summarize these results in terms of the number of people confronted with water scarcities in the future (CI = 4): In 2075, the percentage of world population living in water scarce watersheds is 69% under Scenario M with climate change, and 74% under Scenario M without climate change. However, some 25% of the earth's land area experiences a decrease in runoff, and this occurs in some countries that are already facing severe water scarcity. Moreover, this analysis omits many aspects of possible climate change impacts on water resources. For example, it does not take into account a possible change in interannual and inter-seasonal variability of precipitation and temperature. Moreover, although increased precipitation is likely to increase water availability, it may also increase the rate of flooding in a watershed.

Water uses and water scarcity. The areas of water scarcity identified in this report occur throughout the world, and in both industrialized and developing countries. For current "1995" conditions, the domestic sector accounts for 7.3%, the industrial 18.0%, and the agricultural 74.7% of global water use (under the 10-percentile dry year conditions). In water scarce industrialized countries, the largest user is typically industry, whereas in water scarce developing countries it is almost always agriculture. For year 2075, according to Scenario M, these figures greatly change to 11.2% for the domestic sector, 55.3% for the industrial sector, and 33.5% for the agricultural sector. These results follow from assumptions about the trends in population, economy, and water intensity, and point out the possibility that industry will supersede agriculture as the world´s largest water user.

1. Introduction

Water plays an essential role in the existence of society. Our food supply depends on precipitation collected in an irrigation system or falling directly on a field. In our households water has a central place in day-to-day activities. In industry water is indispensable as a raw material for industrial product, or tool cool combustion processes. Hence, the question, "Is there enough water?" has always been important, and remains so. The problem is that water is not evenly distributed both in time and space. Put another way, the availability of water is not ideally matched to human water needs.

To assess this problem, this paper provides a preliminary estimate of the global distribution of water use and availability, and how this might change over the next 80 years. We examine water quantity, but not water quality. No single report can give a comprehensive picture of the effect of all possible factors on water distribution. Therefore this paper concentrates on a few major driving forces of global change, namely, the effects of population growth, economic growth, climate change, and changes in the intensity of water use. Through the techniques of global modeling and global scenario analysis, we present quantitative estimates of water use and water availability for a specified set of scenarios. In addition to the estimates for present-day conditions, we show water use and availability values for the years 2025 and 2075.

Here, water use is defined as the volume of water withdrawn from surface water or groundwater within a certain year. Water availability refers to the renewable water resources, i.e. the amount of precipitation that is not evaporated or transpirated by plants but becomes runoff. This is the sum of surface runoff and groundwater recharge. Comparing water availability and use on the watershed scale, we determine a freshwater "criticality ratio" as the ratio of use over availability. In addition, we relate this ratio to the water availability per capita, and obtain a freshwater criticality index that describes the degree of water scarcity in the watershed.

In this paper we first briefly describe the model, and then introduce the basic assumptions of the scenarios. Following that, we present key results of our computations of present and future water criticality. In the last section, we describe in detail the global model WaterGAP 1.0 used for the calculations.

2. Overview of WaterGAP model

The global scenario analysis is performed with a new global water model, WaterGAP (**Water** – **G**lobal **A**ssessment and **P**rognosis) Version 1.0, developed at the Center for Environmental Systems Research of the University of Kassel, with assistance from the National Institute of Public Health and the Environment of the Netherlands. The model computes water use and water availability in each of 1,162 watersheds covering nearly the entire terrestrial surface of the world. Fig. A0 in the appendix shows a map of the watersheds. Some aspects of the model´s design and data come from an integrated model of global environmental change called IMAGE 2 (Alcamo et al., 1994a) as well as previous modeling of the global water situation carried out by Klepper (1996). WaterGAP takes into account basic socio-economic factors that lead to domestic, industrial and agricultural water use, and physical and climate factors that lead to river runoff and groundwater recharge. The model is described in detail in Section 5 of this paper. Here we present only a brief overview of its features.

The smallest spatial entity of the model is the grid cell of size 0.5° longitude by 0.5° latitude. The basic calculations are done on the cell level, but model output is aggregated to both the watershed and the country scale. The appropriate scale for assessing freshwater criticality is the watershed scale. Computations are done using different temporal resolutions, depending on the computed variable. Computational results are shown for the years 1995, 2025 and 2075.

"1995" broadly stands for "present-day conditions", as some data from other years were also used. In particular, the climatic conditions of "1995" are the long-term average conditions of the period of 1931-1960.

Water availability and use is not only computed for average precipitation of the respective years, but also for 10-percentile dry years (i. e. precipitation lower than this occurs statistically only once every ten years). The availability in such a year is assumed to be the sum of the surface water runoff produced in the dry year and the groundwater recharge produced in a average precipitation year, as groundwater is stored between years. The water situation in those periodically returning dry years gives a clearer indication of criticality than the situation in average years.

2.1 Water use

Water use calculations for domestic and industrial sectors are based on existing data at the country-scale that are downscaled to the cell scale, and a procedure for scaling these data to the years between 1995 and 2100 according to assumptions about population and economic growth. Water use calculations for agriculture are divided into: (i) livestock water use which is computed from the grid-scale distribution of livestock and their water consumption, and (ii) irrigation water use which is computed from the climate-related consumptive use of crops, and other factors. Both livestock and irrigation water use are computed on the grid-scale.

Water uses in this version of the model are, specifically, *water withdrawals*. Part of the withdrawn water becomes return flow and may be reused by other water users. However, for the estimation of water criticality, it is more appropriate to take into account withdrawal water use instead of consumptive use (difference between withdrawal use and return flow) because
1. instream uses are not considered here
2. the quality of return flow is unknown
3. the location of the water users within the watershed is not known

2.2 Water availability

Version 1.0 of WaterGAP uses a simple approach to compute water availability on a grid-scale that is consistent with the data available on the global scale. WaterGAP 1.0 calculates the daily soil water balance of each grid cell, taking into account physical characteristics of watersheds such as soil, vegetation, slope and aquifer type. Calculations are detailed enough to be tested and calibrated to observed runoff data.

On the watershed scale, water availability is defined as the sum of annual river runoff and groundwater recharge of all the grid cells in the watershed. This is, of course, just a rough approximation of available water supply, since it does not take into account the spatial variability within the watershed nor the month-to-month or week-to-week hydrologic variations. On the other hand, many rivers have reservoirs which store river water from month-to-month, so computing the water availability over an entire year can be a reasonable first indicator of the water situation in a watershed. On the country scale, water availability is computed in the same way as on the watershed scale, and the computed value is therefore equal to the internal renewable resources of the country. With this method, the influence on water availability of watersheds which cross country boundaries is not correctly taken into account.

3. Scenarios

3.1 General features

In this paper we investigate three scenarios of water use and one scenario of water availability.

- The *water use scenarios* include assumptions about the trend in driving forces of water use in domestic, industrial, and agricultural sectors (Table 3.1):

    Scenario M (medium) This is a "best guess scenario" in which intermediate estimates are made for changes in water use.

    Scenario L (low): This contains a set of assumptions that lead to a lower estimate of water use than Scenario M.

    Scenario H (high): This contains a set of assumptions that lead to a higher estimate of water use than Scenario M.

- The *water availability* scenario assumes that average surface temperature and precipitation will change in the future because of climate change. For this paper we use a climate change scenario based on the trend of greenhouse gas emissions given by the IS92a scenario of the Intergovernmental Panel on Climate Change (IPCC). As input to our model, we use temperature and precipitation values computed with the general circulation models of the Max-Planck-Institut and the Geophysical Fluid Dynamics Laboratory.

Although WaterGAP computes changes in water use and availability for the period 1990 to 2100, in this paper we only report calculations for two "time slices" 2025 and 2075.

Table 3.1: Distinguishing assumptions of water use scenarios.

Scenario[*]	Domestic	Industry	Agriculture
L	Water intensity increases with income up to $15,000/cap-yr. Then rapidly declines by 50% and then further to a stringent water conservation target value for domestic water use.	Water intensity is constant with income up to either $5,000 or $15,000/cap-yr. Then rapidly declines by 50% and then further to a stringent water conservation target value for industrial water use.	Irrigated area constant. Water use efficiency improves.
M	Water intensity increases with income up to $15,000/cap-yr. Then declines by 50% and remains constant afterwards.	Water intensity is constant with income up to either $5,000 or $15,000/cap-yr. Then declines by 50% and remains constant afterwards.	New irrigation areas in most developing countries. Water use efficiency improves.
H	Water intensity increases with income up to $15,000/cap-yr. Afterwards, remains constant	Water intensity increases with income up to either $5,000 or $15,000/cap-yr. Afterwards, remains constant	New irrigation areas in most developing countries. Water use efficiency does not improve.

[*]Scenario L = Low, Scenario M = Medium, Scenario H = High

3.2 Basic driving forces of scenarios

Estimating future changes in water use and availability requires a basic set of assumptions about future developments in global population and the global economy. These assumptions are taken from the IS92a scenario of the IPCC. This scenario is one of six scenarios developed by the IPCC to provide a set of feasible global scenarios of greenhouse gas emissions for use in the analysis of climate change (Leggett et al., 1992). In so doing, an international committee of experts agreed upon a set of assumptions about future developments in the growth in population and the economy. In this paper we use population and economic data from IS92a, one of the intermediate scenarios, as the basis for our scenarios. This and other information from the IS92a scenario is only available for 13 world regions. In this paper, we scale all country data within a region by the regional trends in IS92a. Unfortunately, this smoothes out differences in trends between countries.

The assumed trend in population is based on the medium scenario of the United Nations (1991). Assumptions vary substantially from region to region, ranging from a leveling off trend in the coming few decades (or sooner) in industrialized regions, to an increase by a factor of 3.4 in Africa between 1995 and 2075. According to this scenario, global population increases to about 10.4 billion people by 2075 (Table 3.2).

Table 3.2: Regional population assumptions

Region	Population in millions		
	1995	2025	2075
Canada	28	32	31
United States	259	301	296
Latin America	463	672	800
Africa	683	1412	2310
OECD-Europe	375	395	380
Eastern Europe	121	137	142
Former SU	291	328	341
Middle East	235	501	816
India+South Asia	1233	1878	2389
China+C.P.Countries	1404	1838	2020
East Asia	364	554	706
Oceania	22	23	23
Japan	124	132	127
World	5602	8205	10380

Assumptions about economic growth in the IS92a scenario are based partly on earlier IPCC work and partly on short-term estimates of the World Bank (1992). The scenario assumes continuing growth in all regions, ranging from a factor of 3.5 increase of per cap GDP in the United States to a factor of 17 in China over the period from 1995 to 2075 (Table 3.3). Growth of industry as expressed by industrial GDP ranges from a factor of 3.5 for the United States to a factor of 20 for China. Despite the assumed growth, a large income gap remains between industrialized and developing regions.

Table 3.3: Assumptions of per capita GDP and per capita industrial GDP

Region	GDP per capita in 1990 US-$			IGDP per capita in 1990 US-$		
	1995	2025	2075	1995	2025	2075
Canada	23822	43658	90878	8297	15206	31652
United States	25421	45332	89800	7639	13559	26782
Latin America	2719	4958	15210	966	1536	4273
Africa	724	1259	4321	246	545	1736
OECD-Europe	21021	38528	80197	7405	13571	28226
Eastern Europe	2501	8934	16850	1078	3304	6108
Former SU	3408	12231	23068	1757	5821	10592
Middle East	5091	7860	21372	1485	2064	4989
India+South Asia	400	991	4384	111	422	1721
China+C.P.Countries	388	1396	6651	166	824	3335
East Asia	1500	3719	16451	597	1372	5401
Oceania	19021	41274	83872	5576	12009	24323
Japan	27901	60544	123028	11716	25382	51460
World	4431	7314	15685	1562	2661	5528

3.3 Water use assumptions

3.3.1 Domestic water use

Future domestic water use in a country is estimated by multiplying the number of people in a country times its water intensity (water use per capita). Population assumptions are the same for all scenarios, and come from the IS92a scenario described above. Three different scenarios are assumed for changes in water intensity, and all assume that water intensity will change along with changes in income. As an indicator of income we use the Gross Domestic Product per person per year (GDP/cap-yr). Assumptions for changes in GDP/cap-yr come from the IS92a scenario, and the same income assumptions are used for Scenarios L, M and H.

An examination of current domestic water use in different countries shows an upward trend of per cap domestic water use (water intensity) as per cap GDP increases, at least in the range of lower incomes (Fig. 3.1). However, time series data from a few industrialized countries indicate a clear downward trend in the last few years in their total water use. Unfortunately, we do not have independent time series of the sectoral distribution. Therefore, we assume that the temporal changes were the same in each sector. Fig. 3.2 shows the development of per capita domestic water use. The downward trend seems to have occurred only in countries where the annual GDP per capita is above $10,000 to $20,000/cap-yr. Based on these considerations we make the following assumptions about different scenarios, which describe how the country-specific water use intensity changes with change in per capita GDP:

- For Scenario M we assume that the country-specific water intensity of the base year increases with income up to $15,000/cap-yr, and afterwards rapidly declines to 50% of its value at $15,000/cap-year; afterwards water intensity remains constant (Fig. 3.3). The 50% value is reached at a GDP of $18,750/cap-year ($15,000/cap-year + 25%). The rate of increase is given by the best fit line in Fig. 3.1, which was drawn by excluding countries with GDP above $15,000/cap-yr. The development of water use in countries, which were already above a GDP above $15,000/cap-yr in 1990 is adjusted by taking into account the year of maximum water use, while the 25% increase of GDP relates to the actual GDP of

this country in 1990. The GDP turning point of $15,000/cap-year, and the 50% decline should be viewed as only very rough approximations.

- For Scenario H, water intensity increases in the same way as Scenario M up to $15,000/cap-year, but above this point it remains constant (Fig. 3.3).
- For Scenario L, water intensity behaves like in scenario M until it has declined to 50%. Then, it further declines to a stringent water conservation target of 15 m^3/cap-year (Fig. 3.3). This is 38% of the current lowest domestic water intensity of any industrialized country (Switzerland and Great Britain).

Some wealthy countries have decreased water use already to such an extent that scenarios M and H are rather similar.
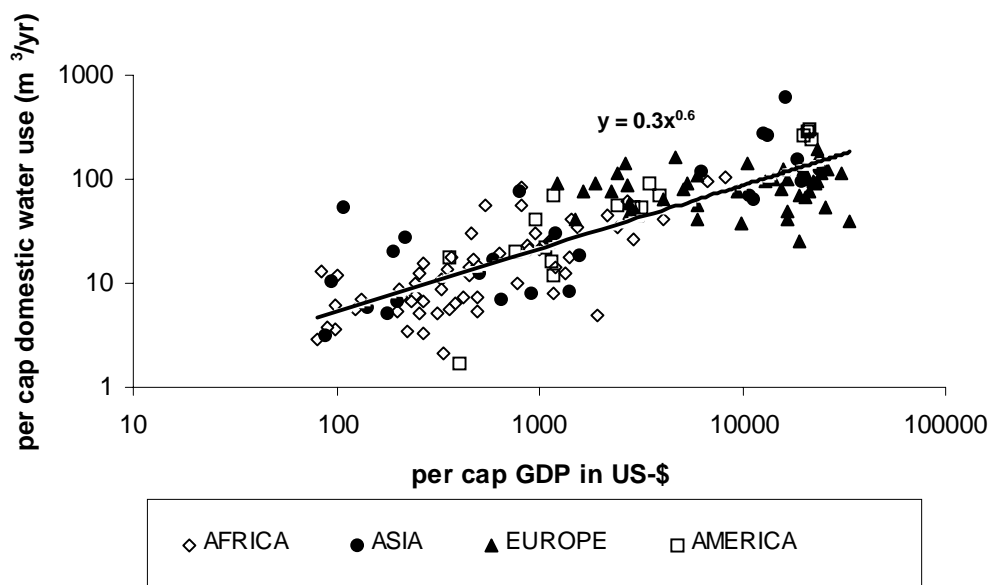
Fig. 3.1: Per cap domestic water use as a function of the per cap GDP. Shown are data from 112 countries (WRI, 1990, 1992, 1994, 1996). The value from the year closest to 1990 was selected for the calculation of the best fit line. Depending on the country, the depicted water use data are from the years 1980 to 1994. The country's per capita GDP is the GDP of the respective year in 1990-US$ (at constant prices) and was derived from data in UN (1995).

Fig. 3.2: Time series of per capita domestic water use in various countries. The GDP/cap-yr range during the respective time period is given in parentheses.

Fig. 3.3: Domestic water use scenarios.

3.3.2 Industrial water use

Future industrial water use in a country is estimated by multiplying the industrial GDP (IGDP) in a country times its water intensity (water use per unit IGDP). The same basic approach is used for industrial water use sce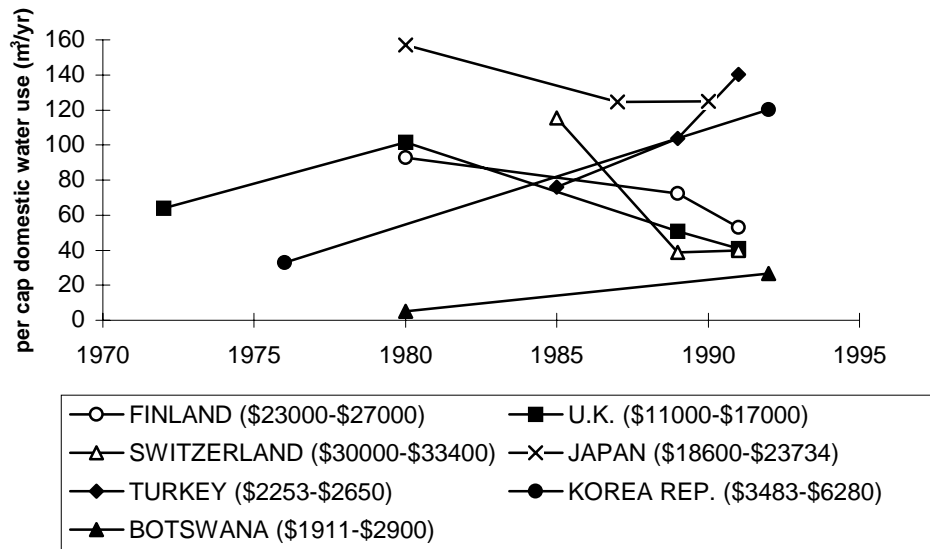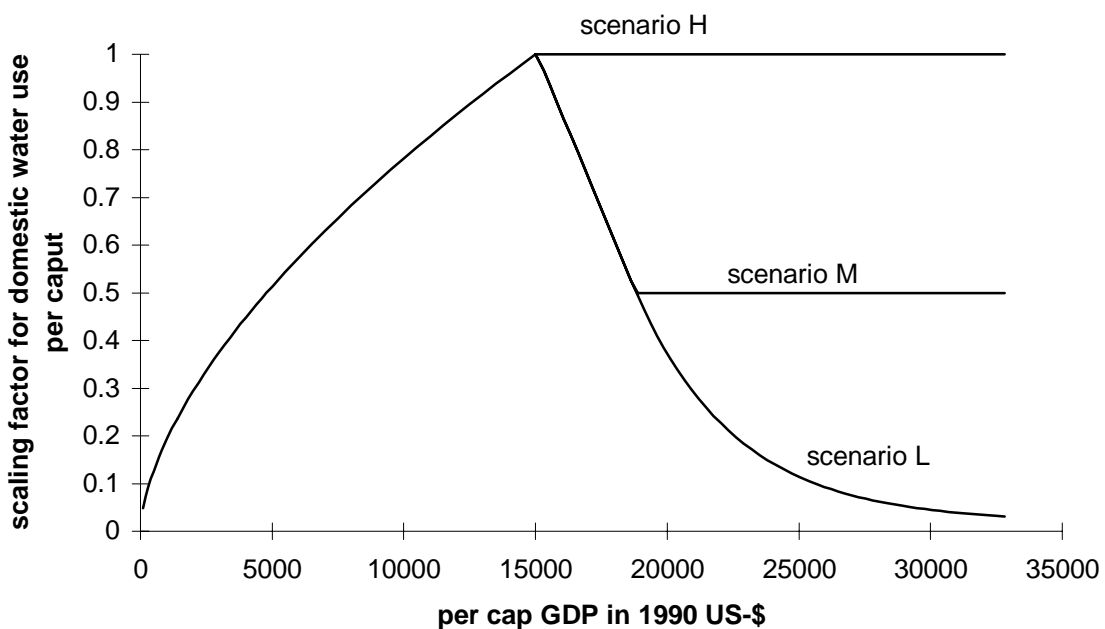narios as was used for the domestic sector. Three different scenarios are assumed for changes in water intensity, and all assume that water intensity will change along with changes in industrial GDP per person per year (IGDP/cap-yr). The reasoning is that as a country becomes more industrialized, the type of industry changes and the approach to using water in industry also changes. The scenario for the change of industrial GDP is taken from the Baseline A scenario of IMAGE 2.1 (Alcamo et al., 1996) for thirteen world regions and then applied to each country within the region. In this scenario, the ratio of industrial to total GDP is assumed to be constant for industrialized countries, but increases in developing countries.

An examination of current industrial water use in different countries shows a slight, but unconvincing trend downward with increasing GDP/cap-yr (Fig. 3.4). On the other hand, we noted above that several industrialized countries have had a clear downward trend in the last few years in their total water use. Moreover, a statistical analysis of available country data provided some evidence that countries with a lower water availability (arbitrarily defined as having less than 1000 m^3/cap-yr) began reducing their industrial water intensity at a GDP/cap-yr roughly around $5000, whereas countries with higher water availability began reducing it at around $15,000 (Kulshreshtha, 1997). Based on these considerations we make the following assumptions for different scenarios, which describe how the country-specific water use intensity as given by the data changes with change in per capita GDP:

- For Scenario M, for countries with higher water availability (arbitrarily defined as equal or above 1000 m^3/cap-yr; values taken from WRI, 1996) we assume that water intensity remains constant at its current level up to an income of $15,000/cap-yr, and afterwards rapidly declines to 50% of its value at $15,000/cap-year (Fig. 3.5). Furthermore we assume that countries with a lower water availability (less than 1000 m^3/cap-yr) have a stronger motivation for conserving water and therefore begin to reduce water intensity at $5,000/cap-yr. After the $5,000/cap-yr point, water intensity in these countries declines as in other countries by 50%.

- For Scenario H, water intensity is simply assumed to remain constant at its current value (Fig. 3.5).

- For Scenario L our approach for the industrial sector is similar to that of the domestic sector. Scenario L follows Scenario M up to 50% decline, then decreases more sharply down to a stringent water conservation target value for industry (Fig.3.5). We assume, that these minimum needs are 25% of the lowest current industrial water intensity in any industrialized country. This amounts to 0.22 m^3/ $100-yr, which is 25% of Denmark´s present industrial water intensity.
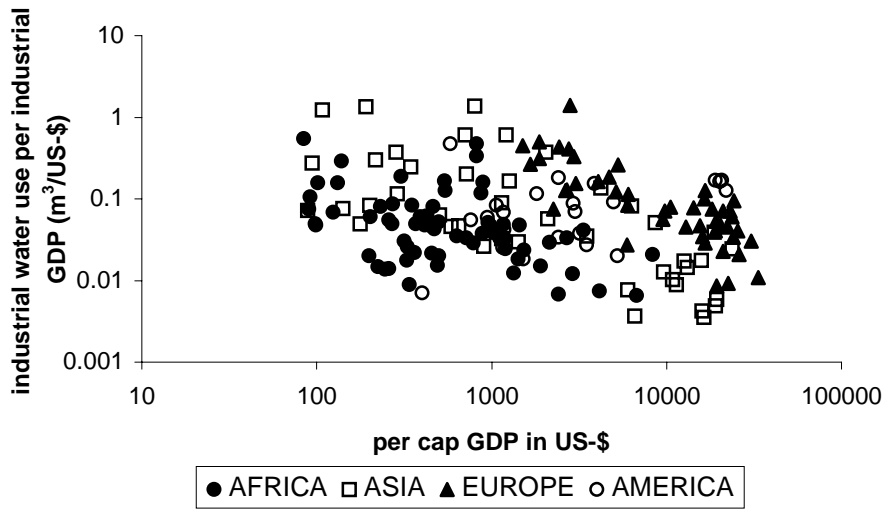
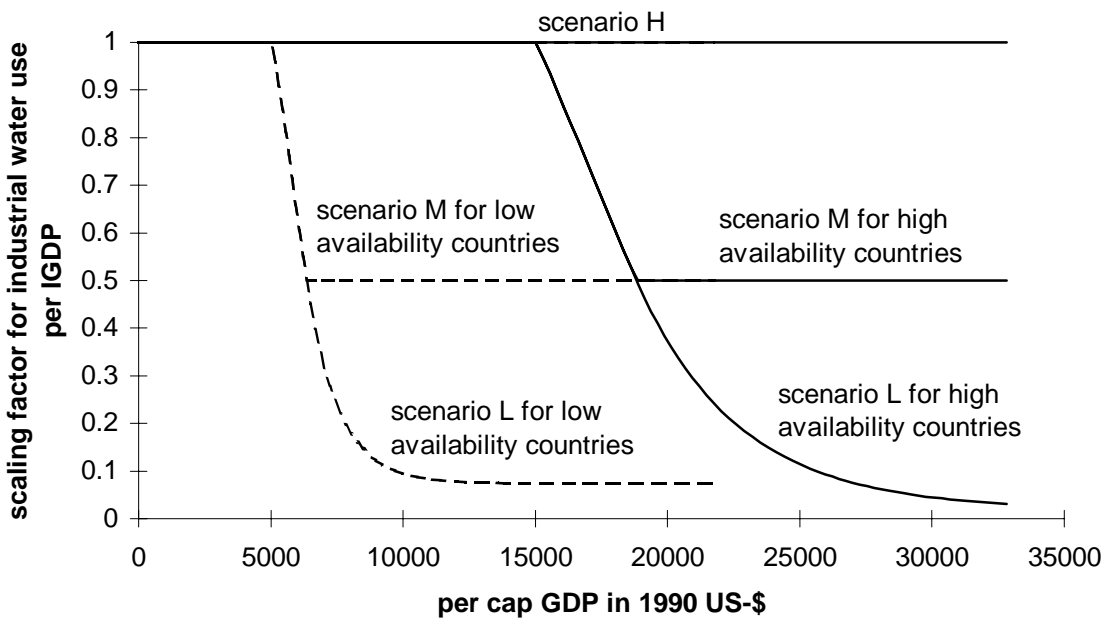Fig. 3.4: Industrial water use per industrial GDP as a function of per capita GDP in 112 countries.

Fig. 3.5: Industrial water use scenarios.

3.3.3 *Agricultural water use*

3.3.3.1 Livestock water use

As noted above, agricultural water use in WaterGAP 1.0 is divided into two parts: water requirements for livestock and water requirements for irrigation. Data on the present density of livestock is provided by NCAR on the GlobalARC GIS Database (1996). Future use of water by livestock is estimated by multiplying the number of livestock animals times the water use per head of livestock (see Section 5.7). To estimate future water use by livestock, we set water use per head constant at its 1995 level (Table 5.1), and change the number of livestock in each country. For the number of livestock we use the estimates for thirteen world regions from the Baseline A scenario of the IMAGE 2.1 model (Alcamo et al., 1996). The Baseline A scenario uses the same assumptions for population and economic growth (from the IS92a scenario) as used in this paper, and is therefore somewhat consistent with other assumptions in this paper. Regional figures from Baseline A are used to scale the 1995 grid-scale density of livestock (described in Section 5.7). The same scenario for future number of livestock is used for Scenarios L, M, and H.

3.3.3.2 Irrigation water use

Future use of water for irrigation is computed by multiplying the number of hectares used for irrigation times the water used per hectare. Both of these variables must be specified for each scenario. We begin with the future extent of irrigated area. Since a detailed calculation of this is very complicated, we make the following simplifying assumptions:
- For developing countries:
    - ⇒ For Scenarios M and H: We assume that the amount of irrigated land increases up to year 2010 according to an FAO study by Alexandratos (1995). (Alexandratos only gives estimates up to 2010). We found that the cereal production estimates of Alexandratos up to 2010 are rather similar to those estimated in the Baseline A scenario of IMAGE 2.1 (described above). Therefore, for the period 2010 to 2075, we scale the amount of irrigated area in each country by the increase in cereal production given in the Baseline A scenario of IMAGE 2.1. We noted above that Baseline A is consistent with the population and economic assumptions made elsewhere in this paper. The resulting increase in irrigated land for years 2025 and 2075 are given in Table 3.4. These assumptions are used for Scenarios M and H. The new irrigated land is allocated to a particular cell based on the algorithm of Klepper (1996) as described in Section 5.7.2.1.
    - ⇒ For Scenario L: we assume no increase in irrigated land.
- For industrialized countries, the amount of agricultural land is already stable or declining. Hence, for Scenarios M, H, and L we assume that the location and extent of irrigated land remains constant at its current situation.

Table 3.4: Assumed change of irrigated area.

world region	irrigated area 2025 / irrigated area 1995	irrigated area 2075 / irrigated area 1995
Canada	1	1
USA	1	1
Latin America	1.60	2.33
Africa*	2.14	3.98
OECD Europe	1	1
Eastern Europe	1	1
former USSR	1	1
Middle East	1.61	2.57
India and South Asia	1.61	2.44
China and centrally planned countries	1.15	1.57
East Asia	1.15	1.57
Oceania	1	1
Japan	1	1

* except Northern African states Egypt, Libya, Tunisia, Algeria, Morocco with 1.59 and 2.95.

The second step in calculating future irrigation water use is to compute the water used per hectare. This is calculated in WaterGAP 1.0 as a function of climate, cropping intensity, and water use efficiency (described in Section 5.7). Hence, these variables must be specified for the scenarios.

For climate data we use results for monthly precipitation and surface temperature, as computed with the climate models of MPI and GFDL, based on the IS92a emissions scenario (see Section 3.4). The same climate scenario is used for Scenarios L, M, and H.

For cropping intensities in developing countries , we use estimates given in Alexandratos (1995) for the year 2010. These estimates are used for Scenarios L, M, and H for the years 2025 and 2075 (Table 5.8). In the developed countries, cropping intensity (like irrigated area) is assumed to remain constant.

Water use efficiency is the remaining variable that is needed to compute irrigation water per hectare. For simplicity, in Scenarios L and M we assume that water use efficiency improves at the same rate in all countries, namely by 0.5%/year. This gives a 16% improvement in water use efficiency for the period between 1995 and 2025, and an 49% improvement from 1995 to 2075. This assumed rate of improvement is in line with estimated future rates of technological improvement of crop yield (see, for example, Alexandratos, 1995, and Alcamo et al., 1996). For Scenario H, no improvement in water use efficiency is assumed.

To sum up the irrigation water use scenario assumptions (see Table 3.1 for an overview):

- For Scenario L, we assume that the amount of irrigated land remains constant at its 1995 level. In addition, we assume that water efficiency improves on all irrigated land.
- For Scenario M, we assume that food production increases in developing countries such that the amount of irrigated land also increases. Water use efficiency improves on all irrigated land.
- For Scenario H, we assume that the amount of irrigated land increases in developing countries. Water efficiency is assumed *not* to improve.

The result of these assumptions is that Scenarios L, M, and H have an increasing level of irrigation water use.

3.4 Water availability assumptions – Climate change scenarios

The precipitation estimates of general circulation models (GCMs) are generally less reliable than their temperature estimates. Therefore, in order to determine the sensitivity of water availability and thus criticality to GCM predictions we use the predictions of two GCMs: The ECHAM4-OPYC model of the Max-Planck-Institut (Röckner et al., 1996), hereafter referred to as the MPI model) and the model of the Geophysical Fluid Dynamics Laboratory (Manabe et al., 1991; Manabe et al., 1992), the GFDL model. The MPI model results are from a transient run based on the IS92a emissions scenario and include the effect of sulfate aerosols; they are more recent than the GDFL model results and therefore probably represent more up-to-date knowledge about climate processes.

In the case of the MPI model, we use the following monthly total precipitation and surface temperature values:
1. the mean of the values of 1950 to 1980 (the climatic normal)
2. the mean of the values of 2020 to 2030 (for the year 2025)
3. the mean of the values of 2070 to 2080 (for the year 2075), when CO_2-equivalent concentrations will have doubled with respect to mean concentrations between 1980 and 1990.

Precipitation in 2025 and 2075 in each 0.5° by 0.5° cell is computed by scaling the precipitation values from the Cramer and Leemans database ($P(CL)$, comp. section 5.3.2) with the total precipitation values of the GCMs (interpolated from the GCM resolution down to WaterGAP resolution):

$$P_{WaterGAP}(2025 \; or \; 2075) = P_{WaterGAP}(CL) \frac{P_{GCM}(mean \; of \; 2020 - 2030 \; or \; 2070 - 2080)}{P_{GCM}(mean \; of \; 1950 - 1980)} \tag{1}$$

Temperature is computed using the GCM surface temperature values as follows:

$$T_{WaterGAP}(2025 \; or \; 2075) = T_{WaterGAP}(CL) + \Delta T_{GCM}$$
$$\Delta T_{GCM} = \left[T_{GCM}(mean \; of \; 2020 - 2030 \; or \; 2070 - 2080) - T_{GCM}(mean \; of \; 1950 - 1980) \right] \tag{2}$$

In the case of the GFDL model, we do not use the GCM results directly to scale our current precipitation and temperature values. Instead, the GFDL results are only used to downscale climate modeling results of Baseline A of IMAGE 2.1, which has similar assumptions to the IS92a scenario, and gives similar emissions (See Section 3.1.3). IMAGE 2.1 contains a two-dimensional climate model which computes temperature and precipitation in 18 latitudinal bands of 10° each, taking into account the different emissions within each zonal band. The cell values of precipitation and temperature at a given time are then obtained within IMAGE 2.1 by scaling the cell values of current precipitation and temperature with both the zonal results of IMAGE 2.1 and the gridded GCM results. For WaterGAP 1.0 simulations of the years 2025 and 2075, we apply the precipitation and temperature values computed by IMAGE 2.1 for 2025 and 2075.

4. Results

4.1 Presentation of results

Scenario results are presented for the years 1995, 2025 and 2075 in two forms:

- As maps showing water availability, water use and the freshwater criticality index on the watershed scale (Appendix A).
- As tables showing water availability, water use, the freshwater criticality ratio and the freshwater criticality index of each country

The tables present information for the various scenarios presented in Section 3. The maps (with the exception of A0 and A1) show results only for the "best guess" scenario of future trends, i.e. changes in water use according to Scenario M, and changes in water availability according to the climate scenario computed by the MPI climate model. In addition, all map information pertains to the 10-percentile dry year (precipitation lower than this occurs only once every ten years). One should also keep in mind that we consider the watershed scale to be the appropriate scale for assessing water criticality, as water is transferred within a watershed but generally not between watersheds. The country values given in the tables in Appendix B, however, do not consider the existence of watersheds, but are a mere summation of all cells within a country.

4.2 Indicators of criticality

Our scenario analysis focuses on the relative abundance or scarcity of water in watersheds and countries. For this purpose we use two simple indicators, the "criticality ratio" and the "criticality index".

- The criticality ratio (CR) is the ratio of water use to water availability in a watershed or country. In both cases it is computed as the sum of grid cell values. Recall that water availability refers to the renewable water resources (the runoff) generated inside the entity of interest. Values for this ratio range from near zero in sparsely-inhabited watersheds where water use is small compared to water availability, to greater than one in arid watersheds where water use is computed to exceed its availability. In the latter case, inhabitants of these watersheds obtain some of their water supply from deep groundwater, from recycled sources, from seawater desalination, from upstream sources, or from elsewhere.
- The "criticality index" (CI) is based on the work of Kulshreshtha (1993) and combines two factors – the criticality ratio and the water availability per capita – into a single indicator of water vulnerability in a watershed and country. The reasoning is that vulnerability increases as two conditions become more critical: (i) total water resources are used up (critical ratio becomes larger), and (ii) the pressure on existing resources increases (water availability per capita declines). The index ranges from 1 for water surplus to 4 for water scarcity, as defined in Table 4.1. To illustrate the use of this index, if one-half of a watershed´s annual water availability is used (criticality ratio = 0.5), and if pressure on water resources is relatively low (water availability per capita is 12,000 m^3/cap yr), then CI = 1, i.e. there is a water surplus. On the other hand, if the criticality ratio is the same, but the pressure on water resources is much greater (for example, if water availability per capita drops to 1,500 m^3/cap yr), then the CR = 3, a much more critical state.

Further details about the criticality indicators are given in section 6.

Table 4.1: Definition of fresh water criticality index (CI)

per cap water availability [m^3/(cap yr)]	criticality ratio (use/availability)			
	< 0.4	0.4 - 0.6	0.6 - 0.8	> 0.8
< 2,000	2	3	4	4
2,000-10,000	1	2	3	4
> 10,000	1	1	2	4

Source: Kulshreshtha, S.N. (1993): World Water Resources and Regional Vulnerability: Impact of Future Changes. RR-93-10, IIASA , Laxenburg, Austria.

1: water surplus
2: marginally vulnerable
3: water stress
4: water scarcity

4.3 The current occurrence of water scarcity

Critical water areas occur on each continent (Figure A12 and Tables B1 and B2). The criticality index is high in arid regions, as expected, but also in densely populated areas of India, China, Europe and the United States, where high water use occurs (Figure A7). If we add up computations from all watersheds, we estimate that 30% of the world's population of 5.6 billion currently live in watersheds with water surplus (criticality index CI=1), while 20% live in marginally vulnerable watersheds (CI = 2), 6% under water stress conditions (CI = 3) and 44% in watersheds that suffer from water scarcity (CI = 4). These percentages refer to conditions in 10-percentile dry years (as explained previously). In years with average precipitation, the percentage living in watersheds with water scarcity drops to 29%.

4.4 The future occurrence of water scarcity

The best guess scenario
While the WaterGAP model Version 1.0 cannot yet give very reliable results for individual watersheds, it can present an overview of possible trends on the global-scale. We compute a "best guess" of future trends by assuming that factors related to water use will change according to Scenario M, and that factors related to water availability will change according to the climate scenario computed with the MPI climate model. Under these scenario assumptions, and under 10-percentile dry year conditions (as explained above), we estimate that the criticality index will tend to increase in more areas of the world than decrease (Figures A13 to A16, and Tables B1 and B2). The percentage of watershed area with critical water scarcity (CI=4) will increase from 31.7% in 1995 to 33.2% in 2025 and 37.3% in 2075. This is despite the increase in runoff in most areas (Figures A5 and A6). Apparently, the growth in water use due to the scenarios of growth in population and the economy is the decisive factor. This can be seen in the maps of annual water use (Figures A7 to A11). The greatest increases in water uses are computed for China, India, Taiwan and the Philippines, where water use is in some areas more than 1000 mm/a higher than in the year 1995. High water use growth rates occur whenever industry is an important water user and industrial GDP grows fast, while the effect of population increase on water use growth (via domestic and irrigation water use) is relatively small. This is illustrated by the water use development in Africa (Figs. A10 and A11). Here, population strongly increases

but not GDP or industrial GDP; hence, the increase in water use in most watersheds is less than 50 mm/a.

One way to summarize the situation is to compute the number of people living in these areas. We estimate that the percentage of the world´s population facing water scarcity (CI = 4) increases from 44% (2.5 billion people) in 1995 to 57% (4.7 billion people) in 2025 and to 69% (7.2 billion people) in 2075. Thus, the affected population affected by water stress is predicted to double by 2025 and to triple by 2075. Note that the percentage of population living in water scarce regions increases much faster than area of these regions. Under average precipitation conditions, these percentages are 29% in 1995, 36.6% in 2025 and 57.8% in 2075.

A higher use estimate

The best guess scenario for water use (Scenario M) assumes that water intensity will substantially decrease in the domestic and industrial sectors, and also that the efficiency of water use in irrigation will significantly increase. By contrast, Scenario H is more pessimistic because it assumes that these improvements do not occur. As a consequence, for almost all watersheds and countries the criticality ratio (use/availability) is higher than under scenario M (Table B3). The differences are largest in countries with a GDP of more than $15,000/cap-yr, as only for these countries, domestic and industrial water use differ for the two scenarios M and H. Model calculations show, however, that water saving under scenario M does not make a big difference on the estimated number of people facing water scarcity in 2025 (Table B3). However, over the longer run in 2075, the two scenarios are quite different. Under Scenario H 78% of the world´s population is faced with water scarcity under dry year conditions (the 10-percentile dry years), as compared to 69% in Scenario M.

A lower use estimate

As compared to the best guess scenario, Scenario L is more optimistic in its assumptions about future water use. For domestic and industrial water use, it assumes a decline to a stringent water conservation target. For agricultural water use, Scenario L assumes that the area of irrigated land remains constant, and that the use of water on this land becomes more efficient.

As can be expected, under scenario L, the criticality ratio of almost all watersheds and countries is lower than under scenario M (Table B3). With respect to the criticality index, stringent water saving shows very positive results for some countries, e.g. Austria, Estonia and Ethiopia (Table B3). On the other hand, most countries that have critical water scarcities (CI = 4) under Scenarios M and H, remain in this category under Scenario L (Table B3). Specifically, the percentage of world population facing water scarcity (CI = 4) in 2025 is 53% under Scenario L, as compared to 57% under Scenario M. In year 2075, the percentage is 61% as compared to 69%. These numbers refer to dry-year conditions (the 10-percentile dry years). In general, while the water conservation of scenario L leads to some improvement in all countries, it does neither radically change the overall global situation nor is it stringent enough to strongly improve the water situation in countries that already today experience water scarcity.

To sum up to this point, the medium water use scenario provides a best guess of future trends, and the low and high scenarios form an uncertainty range around this guess. A robust conclusion from these three scenarios is that the intensity of current water scarcity is not likely to abate in the coming decades, and indeed may affect many more billions in the future.

4.5 The effect of climate change on the water situation

On the global average, the climate change scenario assumed in this analysis leads to increases in both temperature and precipitation. These changes have an opposite effect on water vulnerability because increased temperature leads to greater evapotranspiration, higher agricultural water use, and lower runoff, while increased precipitation leads to lower agricultural water use and higher runoff. From the global perspective, we compute that the annual precipitation effect is more important than the temperature effect, and that overall annual runoff increases and water scarcity is somewhat less severe under climate change. Mean global runoff in a 10-percentile dry year increases from 178 mm/yr in 1995 to 191 mm/yr in 2025 and 211 mm/yr in 2075. We can summarize these results in terms of the number of people confronted with water scarcities in the future (CI = 4): In 2075, the percentage of world population living in water scarce watersheds is 69% under Scenario M with climate change, and 74% under Scenario M without climate change

A somewhat different picture emerges when the spatial variability of these changes are examined (Figure A2 to A6, and Table B5). Depending on the watershed, annual runoff in 2025 is up to 489 mm/yr higher than in 1995, but is also as much as 252 mm/yr lower than in 1995. Increases of more than 50 mm/yr occur in Iceland, on the Norwegian coast, in the Ganges basin in North India, in Bangladesh, Burma, Southern Thailand, Malaysia and most of Indonesia, in Central Africa and parts of Mozambique and Madagascar, in Southeastern Alaska, in the Northwest of South America (including Panama) and in Uruguay and Southern Brazil. Summed up, annual runoff increases in 2025 and 2075 in approximately 75% of the land area with respect to 1995.

The other 25% of the land experiences less runoff, with decreases of more than 50 mm/yr computed to occur in Northern Brazil, Chile, Taiwan and at the Indian west coast. Some countries that already experience severe water scarcity (CI=4) have even less runoff under climate change, such as Cyprus, Israel, Jordan, and Morocco (Table B5). Here, climate change will further intensify the competition for water.

It is also very important to note that this analysis omits many aspects of possible climate change impacts on water resources. For example, it does not take into account a possible change in interannual and inter-seasonal variability of precipitation and temperature. Moreover, although increased precipitation is likely to increase water availability, it may also increase the rate of flooding in a watershed.

An important source of uncertainty in estimating the impact of climate change is the uncertainty of grid-scale precipitation calculations of GCMs. To investigate this uncertainty, we compared WaterGAP calculations using the Max Planck climate model and the GFDL model (see Section 3.4, and Table B5). Indeed, the two models compute considerably different water availabilities for many countries (Table B5). On the other hand, the two models lead to very similar estimates of the number of countries experiencing severe water scarcity (CI=4).

4.6 Water uses and water scarcity

The areas of water scarcity identified in this report occur throughout the world, and in both industrialized and developing countries. Given this situation, which sectors of water use contribute most to water scarcity? For current "1995" conditions, the domestic sector accounts for 7.3%, the industrial 18.0%, and the agricultural 74.7% of global water use (under the 10-percentile dry year conditions). However, these global averages mask differences in water use between industrialized and developing countries: in water scarce industrialized countries, the largest user is typically industry, whereas in water scarce developing countries it is almost always agriculture (Table B4).

For year 2075, according to Scenario M, these figures will greatly change to 11.2% for the domestic sector, 55.3% for the industrial sector, and 33.5% for the agricultural sector. These results follow from assumptions about the trends in population, economy, and water intensity, and point out the possibility that industry will supersede agriculture as the world´s largest water user. This is because of the assumed industrial growth in developing countries. In industrialized countries, the industrial sectors continue to have the highest use, and in developing countries the industrial and domestic sectors sometimes exceed agricultural water use (Table B4).

From this global perspective, special attention should be given to the agricultural sector in the coming decades, but more effort in the future should be devoted to other sectors. However, we must stress that this order of priorities for water conservation could very well change once cultural and economic factors are included in this picture.

5. Detailed description of the WaterGAP 1.0 model

WaterGAP 1.0 consists of
- a module to compute water availability, the hydrological model that computes runoff (comp. section 5.3), and
- a module to compute withdrawal water use, the water use model (comp. section 5.4).

Fig. 5.1 provides an overview of the model system and its inputs and outputs.

5.1 Spatial resolution

The land mass of the earth is represented by a 0.5° by 0.5° grid, which results in 59831 cells. Each cell is part of a watershed, of a country and of a world region. For most freshwater related problems, the watershed is the appropriate entity. However, some data are only available on the country or world region scale. The cell-based calculations allows any necessary or desirable translation between spatial entities like countries or watersheds. 1162 watersheds of widely varying size are distinguished. The watershed boundaries were obtained from Klepper (1996) who corrected those identified by Lozar (1992, in GlobalARC GIS Database, 1996), in particular the European ones. In addition, Klepper subdivided larger basins into smaller ones. Fig. A0 in the appendix shows a map of the watersheds.

One problem with the current land mask is that large freshwater lakes with a size of grid cell or larger are not included in the grid and thus in the calculations. For watersheds which include such lakes, water availability might be overestimated as evaporation from large water bodies tends to be larger than precipitation onto them.

5.2 Temporal resolution

Simulations are performed for 1995, 2025 and 2075. Here, the year 1995 stands for "present-day conditions", not exactly for the actual year 1995, as data from a variety of years were used. For each year of interest, the hydrological model is run with daily time steps; however, climatic input (temperature, precipitation and cloudiness from the CLIMATE data base of Cramer and Leemans (van Woerden, 1995) is only available as monthly mean values which are interpolated to daily values. The climatic input data represent long-term climatic averages. For model output representative of present-day conditions (year 1995), the model is run with these input data over two years when an equilibrium is reached. For the years 2025 and 2075, the CLIMATE data base value are modified according to predictions of General Circulation Models (GCM). Consumptive use of irrigation is equally computed on a daily basis, while all the other water use components are computed just once per year of interest.
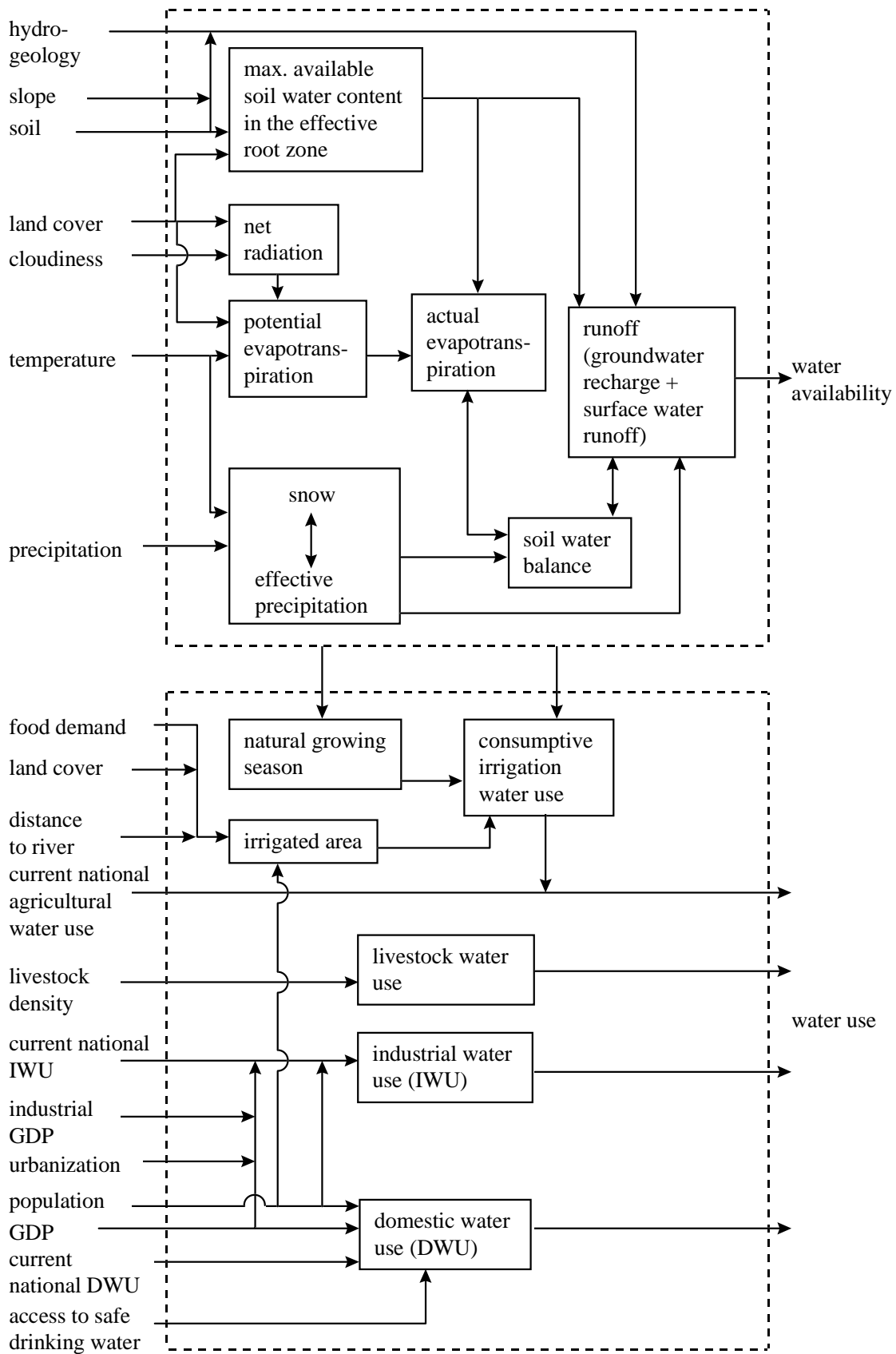
Fig. 5.1: Overview of inputs and processes in WaterGAP 1.0.

5.3 Water availability - The hydrological model

5.3.1 Water balance at the grid cell scale

$$\frac{\partial S}{\partial t} = P_{eff} - E_a - R \qquad (3)$$

S = actual water content of the soil within the effective root zone [mm]
P_{eff} = effective precipitation [mm/d]
E_a = actual evapotranspiration [mm/d]
R = runoff [mm/d]
t = time [d]

Total runoff R is partitioned into surface and fast subsurface runoff R_s and slow groundwater runoff (or base flow) R_g.

$$R = R_s + R_g \qquad (4)$$

The effective precipitation P_{eff} is the sum of rain and meltwater. From the available total precipitation P and temperature T, P_{eff} is computed applying the following snow model:

$$
\begin{aligned}
&P_{eff} = 0 \\
&\frac{\partial S_s}{\partial t} = P - E_p \qquad &\text{if } T \leq T_t
\end{aligned}
$$

$$
\begin{aligned}
&P_{eff} = P - \frac{\partial S_s}{\partial t} \\
&\hspace{3cm} \text{if } T > T_t \text{ and } S_s > 0 \\
&\frac{\partial S_s}{\partial t} = K_s(T - T_t)
\end{aligned}
$$

$$P_{eff} = P \qquad \text{if } T > T_t \text{ and } S_s = 0 \qquad (5)$$

T = temperature [°C]
S_s = snow-water equivalent [mm]
T_t = threshold temperature [°C] (0°C)
E_s = sublimation [mm/d]
K_s = degree-day factor [mm/(d °C)]

Based on a large number of model applications in Sweden by Bergström (1990), a threshold temperature of 0°C is chosen, while 2 mm/(d °C) is used for the degree-day factor in the case of forests and 4 mm/(d °C) in the case of other landcover (comp. Table 2.1)

5.3.2 Precipitation

Cramer and Leemans derived a data set of long-term mean monthly terrestrial precipitation values on a 0.5° by 0.5° grid using measured monthly precipitation from 1931 to 1960 at about 16000-20000 stations (van Woerden, 1995), using at least data from five years within this period. They applied the Hutchinson interpolation algorithm (Hutchinson, 1995), which takes into account topography. From the monthly values, we calculated daily ones by linear interpolation.

An important consideration in water resources assessment is variability. Water availability should meet water demand not only in average years, but also in dry years. In general, variability of runoff is higher than variability in precipitation. Dry years are particularly critical in areas with irrigated agriculture where irrigation water demand is higher in these years. For the computation of a water criticality index, one should therefore not only look at average monthly conditions but more critical ones with lower than average precipitation values. However, to our knowledge, there do not exist long-term estimates of interannual variability of monthly precipitation. There is, however, a rather old map of long-term annual precipitation variability. This global map of Biehl (1943) (given in Riehl, 1979), which shows the coefficient of variance C_v of annual precipitation in seven classes ("below 10%" to "over 40%"), was digitized by Klepper (1996) and was kindly provided to us. Assuming that annual precipitation is normally distributed, we computed the precipitation of a 10-percentile dry year P_{10d} (i.e. only 1 in 10 years has less precipitation) as follows from the mean precipitation values $P_{average}$ of Cramer and Leemans:

$$P_{10d} = P_{average}\left(1 - 1.28\,C_v\right) \tag{6}$$

5.3.3 Temperature

Similar to precipitation, Cramer and Leemans determined a dataset of long-term mean monthly terrestrial air temperature (van Woerden, 1995). Daily values are obtained by using cubic splines. Temperature variability is not taken into account.

5.3.4 Evapotranspiration and sublimation

Evapotranspiration is the combined water loss from the soil due to evaporation directly from the soil and transpiration of soil water via plants (root water uptake). Sublimation refers to the phase change of water from snow to atmospheric vapor.

Of the many approaches to compute evapotranspiration, the Penman-Monteith equation (Shuttleworth, 1993) appears to be suited best as it includes the main driving forces of evapotranspiration: net radiation, temperature, vapor saturation deficit of the air and wind velocity. The diffusional resistances of the plant surface and the atmospheric boundary layer are parameterized by a stomatal and an aerodynamic resistance. Following Jarvis (1976), stomatal resistance is a function of leaf area index, net radiation, temperature, saturation deficit of ambient air, leaf water potential (taken to be expressed as soil moisture potential or soil water content) and external concentration of CO_2. Aerodynamic resistance is computed as a function of vegetation height and wind velocity. According to Penman-Monteith, actual evapotranspiration [mm/d] is

$$E_a = \frac{1000}{L\rho_w} \left[\frac{s(R_n - G) + \rho_a c_p D / r_a}{s + \gamma(1 + r_s / r_a)} \right] \qquad (7)$$

L = latent heat of evaporation [J/kg]
      = $(2.501 \cdot 10^6 - 2361 * T)$ J/kg
ρ_w = density of liquid water [kg/m^3]
s = increase of saturated vapor pressure with temperature [Pa/K]
      = $2.503 \cdot 10^6 \exp[17.269 \, T_c /(237.3 + T_c)]/(237.3 + T_c)^2$ Pa/K
γ = psychrometric constant [Pa/K]
R_n = instantaneous net radiation [J/(d m^2)]
G = heat flux from/to soil [J/(d m^2)]
ρ_a = density of air [J/(kg K)]
c_p = specific heat of moist air [kg/m^3]
D = vapor pressure (or saturation) deficit (saturated vapor pressure minus actual vapor
      pressure) [Pa]
r_s = surface (or stomatal) resistance [d/m]
r_a = aerodynamic resistance [d/m]

With the Penman-Monteith equation, the negative feedback processes between plant behavior and atmospheric variables (e.g. vapor saturation) as described by McNaughton and Jarvis (1991) can be taken into account in a coupled model of the atmosphere, vegetation and soil. However, if evapotranspiration is computed with fixed atmospheric boundary conditions, as is done in WaterGAP, the feedbacks are neglected, and thus the influence of vegetation on evapotranspiration will be overestimated. The main reason for not using the Penman-Monteith equation in WaterGAP 1.0 is that there are not enough measurement values of vapor saturation and wind velocity available to produce datasets of climatic averages of the variables at the required spatial resolution. The Priestley-Taylor equation is instead chosen here to compute potential evapotranspiration E_p, which is defined as the evapotranspiration that occurs if evapotranspiration is not restricted by moisture availability. The original Priestley-Taylor equation has been shown to successfully predict evapotranspiration from well-watered lysimeters in humid regions, and has been modified for use in arid regions (Jensen et al., 1990). Actual evapotranspiration under restricted water availability is then computed from potential evapotranspiration as a function of soil water content.

Evapotranspiration from the soil is assumed to occur only at temperatures above 0°C, while sublimation from snow only happens at 0°C and below.

5.3.4.1 Potential evapotranspiration

Priestley and Taylor (1972) evaluated measured evaporation over well-watered vegetation and over open water bodies when advection of air was negligible. They reason that at a larger scale the effect of advection over land will be generally minor, and that thus the evaluation of the plot scale events without advection is applicable to the grid-scale under most circumstances. Their measurements were all done in humid regions. Following Priestley and Taylor, potential evapotranspiration E_p is computed as

$$E_p = \alpha \frac{1000}{L\rho_w} \left[\frac{s(R_n - G)}{s + \gamma} \right] \qquad (8)$$

where $\alpha = 1.26$. Obviously, Eq. 8 can be derived from Eq. 7 if stomatal resistance r_s goes to infinity and the vapor saturation deficit related term is 0.26 times as large as the radiation related term. Jensen et al. (1990) tested a large variety of evaporation formula against evaporation from well-watered lysimeters. For the five lysimeters in humid regions, Priestley-Taylor equation gave very good agreement, while for the six lysimeters in semi-arid and arid areas, a mean α of 1.74 gave a better fit. This was explained by heat advection to the well-watered (irrigated) lysimeters. Thus, it is not clear, whether a value of 1.74 is adequate at the grid scale. Shuttleworth (1993) recommends to set $\alpha = 1.26$ for humid areas with relative humidity of 60% or more (error +-15%, Shuttleworth, 1993, p. 4.17 and 4.21), and $\alpha = 1.74$ for other areas. Shuttleworth (1993) states that now more substantial evidence supports this empirical relationship on a regional average for regions with uniform vegetation cover or with land cover which is heterogeneous at the scale of a few kilometers, if E_p is considered to be reference crop evaporation E_{rc}. Then, the crop/forest specific evapotranspiration without soil moisture stress could be computed using Eq. 8 and potential crop coefficients K_{co}. In WaterGAP 1.0, potential evapotranspiration is assumed to be independent of vegetation. However, arid and humid areas of the globe are distinguished based on the potential vegetation as computed by IMAGE 2.1 (Table 5.1), such that their extent and that of the areas with relative humidities above and below 60% correspond approximately.

For the temporal scale of interest in WaterGAP 1.0, soil heat flux G can be neglected (Shuttleworth, 1993, p. 4.10). The net radiation R_n is the sum of the net short-wave radiation (difference between incoming and reflected short-wave solar radiation) and the net long-wave radiation (difference between the incoming and the outgoing long-wave radiation). Daily net radiation R_n is computed as a function of the day of the year, latitude, cloudiness and short-wave albedo following Shuttleworth (1993), except for the computation of the sunset hour angle which is better approximated by the CBM model of Forsythe et al. (1995). Cloudiness is provided by the CLIMATE database (Cramer and Leemans, cited in van Woerden, 1995). Albedo is taken to be a function of landcover as assigned by IMAGE 2.1 (Table 5.1). Whenever a cell is snow-covered, an albedo of snow of 0.40 is used; this value is set to a rather low value for snow because in reality, a cell might only be partly snow-covered.

Table 5.1: Potential evapotranspiration coefficient and rooting depth.

Potential vegetation (landcover) class of IMAGE 2.1	α in Priestley-Taylor equation as a function of potential vegetation	short-wave albedo (values similar to those used in IMAGE 2.1)	rooting depth [m] as a function of landcover
tundra	1.26	0.20	0.5
wooded tundra	1.26	0.15	1.0
boreal forest	1.26	0.13	2.0
cool coniferous forest	1.26	0.11	2.0
temperate mixed forest	1.26	0.11	2.0
temperate deciduous forest	1.26	0.13	2.0
warm mixed forest	1.26	0.11	2.0
steppe	1.74	0.25	1.0
hot desert	1.74	0.35	0.1
shrubland	1.74	0.22	1.5
savanna	1.26	0.16	1.5
tropical woodland	1.26	0.11	2.0
tropical forest	1.26	0.07	2.0
(agricultural land)	n.a.	0.23	1.0
(regrowth forest)	n.a.	0.15	2.0
(urban areas, major cities)	n.a.	0.15	1.0

* n.a.: not applicable

5.3.4.2 Actual evapotranspiration

Actual evapotranspiration E_a is computed as a function of potential evapotranspiration E_p, the actual water content of the soil in the effective root zone S and the total available soil water capacity in the effective root zone S_{max}. The smaller E_p, the smaller can the ratio of water content in the soil and total available water capacity become before E_a drops below E_p.

$$E_a = \min\left(E_p, E_{p\max} \frac{S}{S_{\max}} \right)$$

(9)

E_{pmax} = maximum potential evapotranspiration [mm/d] (9.5 mm/d)
S_{max} = total available soil water capacity within the effective root zone [mm]

S_{max} is computed as the product of the total available water capacity in 1 m soil TAWC from Batjes (1996) and the vegetation-specific rooting depth. The arithmetic mean TAWC of each cell is used; it ranges between 30 and 300 mm. Glaciated areas are not given any TAWC value and are thus not included in the calculation of water availability. Rooting depth values are assigned to landcover classes as used in IMAGE 2.1 (Table 5.1).

5.3.4.3 Sublimation

If temperature is at or below the threshold temperature, evapotranspiration is assumed to be zero, while sublimation occurs if snow is present. Sublimation is computed like potential evapotranspiration using the Priestley-Taylor approach (with $\alpha = 1.26$) but using the latent heat of sublimation ($2.83 \cdot 10^6$ J/kg) instead of the latent heat of evaporation. That sublimation can be an important part of the hydrological cycle is shown by Marks and Dozier (1992) who measured 500 mm sublimation out of a total of 2500 mm precipitation as snow in the Southern Sierra Nevada, California.

5.3.5 *Runoff*

Total runoff R is computed as

$$R = P_{eff} \left(\frac{S}{S_{\max}} \right)^{\gamma} \qquad \text{(HBV approach; Bergström, 1994)} \qquad (10)$$

γ = runoff factor that is varied in the course of calibration

Total runoff R is partitioned into surface and fast subsurface runoff R_s and slow groundwater runoff (or base flow) R_g such that

$$\begin{aligned} R &= R_s + R_g \\ &= (1 - f_g)R + f_g R \end{aligned} \qquad (11)$$

f_g = fraction of total runoff which recharges the groundwater [-]

5.3.5.1 *Slow groundwater runoff*

On the cell scale, groundwater runoff is conceptually equal to groundwater recharge. Groundwater recharge is computed following Klepper (1996); all the input data files were provided by him.

The fraction f_g of total runoff which recharges the groundwater and contributes to baseflow is assumed to be a function of soil texture, slope and aquifer type. Thus, for a given cell, groundwater recharge is a constant fraction of runoff; however, total runoff is limited by a maximum groundwater recharge value R_{gmax} that depends on soil texture.

$$R_g = \min(R_{g\max}, f_g R)$$
$$with \qquad (12)$$
$$f_g = f_t f_s f_a$$

f_t = texture-related factor [-]
f_s = slope-related factor [-]
f_a = aquifer-related factor [-]

Soil texture and slope are derived from the UNESCO Soil Map of the World (1974) at a resolution of 1/12° by 1/12°, in which both parameters are divided into three classes (Table 5.2). The soil texture refers only to the uppermost 30 cm of the soil. Cell-specific texture and slope values (on a 0.5° by 0.5° resolution) were computed as the arithmetic mean of the 1/12° values, such that values between 10 and 30 result for both texture and slope. For each of the three texture classes, typical values for R_{gmax} and f_t are assigned, while for each slope class, a typical value of f_s is given (Table 5.2). These values are expert guesses. Cell-specific values of R_{gmax}, f_t and f_s were computed by interpolating the values according to the cell-specific texture and slope values.

Table 5.2: FAO texture and slope classes with the values assigned to them in WaterGAP (from Klepper, 1996).

FAO soil texture class	texture value	R_{gmax} [mm/d]	f_t
coarse: sands, loamy sands and sandy loams with less than 15% clay and more than 70% sand	10	3	0.95
medium: sandy loams, loams, sandy clay loams, silt loams, silt, silty clay loams and clay loams with less than 35% clay and less than 70 % sand; the sand fraction may be as high as 85% if a minimum of 15% clay is present	20	1.5	0.75
fine: clays, silty clays, sandy clays, clay loams and silty clay loams with more than 35% clay	30	0.75	0.25

FAO slope class	slope value	f_s
level to gently undulating: dominant slopes 0-8%	10	0.75
rolling to hilly: dominant slopes 8-30%	20	0.20
steeply dissected to mountainous: dominant slopes > 30%	30	0.05

Aquifer types were derived from a hydrogeological map of Europe (IAH, 1974-1990) and of Africa (UN, 1988), and a geological map of the world based on Bederke and Wunderlich (1968) and Dierke (1975). The hydrological maps were digitized at RIVM, the Netherlands, while the last map was provided in electronic form by Wolters-Noordhoff B.V. Six aquifer types are distinguished. Geologic maps show the age of the rocks and furthermore differentiate intrusive and effusive igneous rocks, but do not directly show the rock type (e.g. consolidated sedimentary rock, fissured metamorphic rock), which would be indicative of the hydrogeological behavior. However, there exists some correlation between the units in geological maps and the hydrogeologically relevant rock type, which was derived here from comparisons of the geological map to the hydrogeological maps of Africa and Europe. There was a fairly good correspondence between the hydrogeological map of Africa and the geological map of Africa, while the correspondence of the hydrogeological and geological maps of Europe was less accurate. This is probably the result of the fact that the African hydrogeological map is actually a re-interpretation of (another) geological map, while the European map provides primary material. Thus global aquifer types were based on the correspondence between the geological units of the geological map of the world and the aquifer types of the African hydrogeological map. The resulting global hydrogeological map is rather coarse (with a resolution of ca. 2° by 2°).

Like the texture- and slope-related factors, aquifer-specific values of f_a are "just" expert guesses. Klepper and colleagues derived values of f_a for Africa, while other researchers (Meinardi et al.) from the RIVM derived such values for Europe (

Table 5.3). Differences between the two parameter sets are explained by the deeper weathering under warm and humid conditions. Klepper (1996) then suggests to obtain cell-specific f_a-values by interpolating between the two parameter sets based on annual cell temperature. The values of Europe are valid for an average of 10°C, while the values for Africa represent an average of 25°C. In order to avoid unrealistic values, the limits for f_a are set to 0.05

and 1. In the future, the soil-, texture- and aquifer-related factors will be calibrated by analysing base flow measurements.

Table 5.3: Aquifer types and corresponding values of f_a (table modified from Klepper, 1996).

aquifer unit	description	corresponding European aquifer unit	f_a (Africa)	f_a (Europe)
1	Tertiary: unconsolidated sedimentary aquifers of good permeability	Tertiary: unconsolidated sedimentary aquifers of good permeability plus brackish aquifers	1.00	0.95
2	Quaternary: unconsolidated sedimentary aquifers of medium to poor permeability	Quaternary: unconsolidated sedimentary aquifers of medium to poor permeability	0.80	0.80
3	Paleozoic: consolidated sedimentary aquifers of good permeability	Paleozoic: consolidated sedimentary aquifers and fissured igneous and metamorphic rocks	0.95	0.40
4	Mesozoic: consolidated sedimentary aquifers of medium to poor permeability	Mesozoic: consolidated sedimentary aquifers of medium to poor permeability	0.80	0.70
5	Cenozoic and Mesozoic volcanic rocks	Cenozoic: volcanic rocks	0.90	0.50
6	Precambrian: igneous and metamorphic rocks of low to negligible permeability	Precambrian: igneous and metamorphic rocks of low to negligible permeability	0.70	0.10

5.3.5.2 *Fast surface and subsurface runoff*

Fast surface and subsurface runoff is computed as the difference between total runoff and groundwater runoff.

5.3.6 *Urban areas*

In urban areas, the soil is partially sealed to infiltration, such that surface runoff increases while evapotranspiration and groundwater recharge decrease. The extent of this effect does not only depend on the degree of sealing, but on the type and location of the sealing material and the sewer system. While in the city centers typically 85-100% of the areas are sealed, in residential areas with single family units, it may be 10% to 50%. In WaterGAP 1.0, 380 out of 59831 cells are urban. As a first guess, it is assumed that 10% of the urban cell area is sealed in such a way

that the precipitation turns into surface runoff immediately. Only the remaining precipitation is partitioned into evapotranspiration, surface and groundwater runoff.

5.3.7 Routing between grid cells

Routing between grid cells is not implemented in WaterGAP 1.0. The water availability within a watershed is computed by summing up the cell values of surface and groundwater runoff. This sum can be considered to be equivalent to the discharge at the mouth of the watershed.

5.3.8 Preliminary calibration to annual discharge of large rivers and regionalization

5.3.8.1 Calibration

Hydrologic models require calibration to measured river discharge even though they are physically based models in which a variety of independently determined data is used (e.g. soils and vegetation data). Consistent with our goal to compute annual water availability, consistent with the long-term mean climate data and consistent with our model that does not take into account routing, we calibrate the runoff coefficient γ in Eq. 10 by comparing computed total annual runoff against long-term annual means of measured river discharge. The computational value is the sum of all cell values of total runoff (Eq. 10) within all the watersheds that drain to the respective measurement point of river discharge.

We cannot, however, use measurement data of river basins of which the digital representation appears to be inconsistent with topographic maps. A further prerequisite is that the measurement station is close to the mouth of one of the digitized subbasins of the river basin (compared to the total size of the basin). We have chosen 43 large river basins on the five continents for which long-term discharge measurements are available. They cover 33% of the total land surface of the earth. For 39 rivers, discharge data from the GRDC (Grabs et al., 1996) are used, while for four, data from Probst and Tardy (1987, as cited in Gleick, 1993, p. 149) are taken. Table 5.4 lists the rivers and measurement stations and periods as well as the given river basin areas and mean annual discharges. The WaterGap watersheds are combined to larger units corresponding to the drainage area of the measurement point where necessary. The thus obtained watershed areas can differ significantly from the areas given in the literature. While for 19 basins, the difference is less than 10 %, the Senegal and Nile river basin areas differ by more than 65%; for such dry basins, it is difficult to determine the exact drainage area. For all basins except the Guadalquivir, the WaterGAP basins appear to be reasonably similar to the basin area that can be deduced from maps.

By trial-and-error, a good fit of the annual discharge of 38 of the 43 basins was obtained by using the γ-values listed in Table 5.4, which range between 0.05 and 9.5. The higher the γ, the lower the computed runoff. The arithmetic mean of γ is 1.8. For only five of the 38 basins, a γ larger than 3 was fitted. These are relatively dry basins with a ratio of annual precipitation over annual potential evapotranspiration $E_p/P > 2$ (except the Loire).

However, for five river basins (Murray, Nile, Niger, Senegal, Don), the WaterGAP 1.0 hydrological model considerable overestimates runoff, no matter how large γ is. All of these basins except the Don basin are very dry basins with $E_p/P \geq$ ca. 3 (Only the Indus basin has an equally high E_p/P but a low γ). In the case of the Murray, this is probably due to an underestimation of the available water capacity in the root zone S_{max} ; in the model, too much runoff occurs in winter, when E_p is close to zero, which could be precluded by a value of S_{max} which is approx. twice the assigned value of ca. 80 mm. The situation is different in the three African basins of the Nile, the Niger and the Senegal. The overprediction of runoff of at least the

first two rivers is due to the fact that our hydrological model cannot simulate correctly the huge swamps which evaporate a large percentage of the runoff produced in upstream regions; averaged over the (long-term mean) year, in our model a cell can only evaporate what it receives as precipitation. These swamps, however, receive water horizontally from the river (i.e. from neighboring cells), which then evaporates at a high rate. For each of the five river basins, Table 5.4 lists the factor F_c by which the discharge computed with $\gamma = 10$ has to be divided in order to match the measured discharge.

Table 5.4: Calibration of runoff coefficient γ of Eq. 10 to measured annual discharge. Measurement data from GRDC (Grabs et al., 1996) except where noted.

river	station	latitude (+ N, - S)	longitude (+ E,- W)	basin area [1000 km^2]	measurement period	mean annual discharge [m^3/s]	mean annual runoff [mm/a]	river basin area in WaterGAP [1000 km^2]	runoff coefficient γ to fit discharge	E_p / P
Amazon	Obidos	-1.9	-55.5	4640	1928-1983	155432	1056	5155	0.8	1.14
Parana	Corrientes	-29.97	-58.85	1950	1904-1983	16358	265	2093	1.9	1.56
Orinoco	Puente Angostura	8.15	-63.6	836	1923-1987	31061	1172	967	0.8	1.03
Magdalena	Calamar	10.27	-74.92	257	1971-1979	6974	854	275	0.9	1.05
Parnaiba	Porto Formosa	-3.47	-42.5	290	1963-1975	785	85	320	9.5	2.11
Uruguay	Concordia	-31.40	-58.02	249	1968-1979	5218	660	350	1.5	1.07
Brazos	Richmond	29.58	-95.53	117	1965-1984	200	54	141	1.9	2.65
Mississippi	Tarbert Landing	31.02	-91.62	3924	1965-1984	14703	118	3466	1.7	1.75
Fraser	Hope	49.38	-121.45	217	1912-1990	2709	394	183	0.05	1.41
Columbia*	The Dalles	45.6	-121.7	614	1879-1982	5452	280	648	0.1	2.86
Santiago	El Capomal	21.83	-105.12	129	1965-1981	291	71	141	3.7	2.56
Murray	Lock 9 Upper	-34.18	141.6	991	1965-1984	257	8	1038	no fit; with = 10, F_c = 3.23	3.90
Burdekin	Clare	-19.77	147.23	130	1965-1984	360	88	138	2.1	3.06
Zaire	Kinshasa	-4.3	15.3	3475	1903-1983	40250	3653	2797	1.4	1.39
Nile*	Aswan	24.1	32.9	1500	1800-1976	2830	59	2497	no fit; with = 10, F_c = 1.27	2.93
Niger	Gaya	11.88	3.4	1000	1952-1990	1153	36	733	no fit; with = 10, F_c = 2.25	3.21
Senegal	Dagana	16.5	-15.5	268	1903-1974	691	81	476	no fit; with = 10, F_c = 1.80	3.62
Zambezi*	Matundo-Cais	-15.85	33.58	940	1925-1983	2429	82	984	5.2	2.20
Rufiji	Stigler	-7.80	37.9	158	1954-1978	790	157	134	1.7	2.32

* Probst and Tardy (1987), cited in Gleick (1993).

Table 5.4 continued.

river	station	latitude (+ N, - S)	longitude (+ E, - W)	basin area [1000 km^2]	measurement period	mean annual discharge [m^3/s]	mean annual runoff [mm/a]	river basin area in WaterGAP [1000 km^2]	runoff coefficient γ to fit discharge	E_p / P
Amur	Komsolmolsk	50.63	137.12	1730	1933-1984	9739	178	1995	0.9	1.51
Yenisei	Igarka	67.48	86.5	2440	1936-1984	17847	231	2318	0.3	1.35
Olenek	Mouth of Pur	72.12	123.22	198	1965-1984	1000	159	157	0.05	1.61
Ob	Salekhard	66.57	66.53	2950	1930-1984	12504	134	2947	0.9	1.52
Lena	Kusur	70.7	127.65	2430	1935-1984	16622	216	2243	0.2	1.48
Godavari	Polavaram	16.92	81.78	299	1901-1979	3061	323	337	1.7	1.92
Ganges	Farakka	25.0	87.92	935	1949-1973	12037	406	976	1.8	1.60
Indus	Kotri	25.37	68.37	832	1973-1979	2396	92	830	0.8	4.52
Brahmaputra	Bahadurabad	25.18	89.67	636	1969-1975	19674	975	514	0.05	0.95
Chao Phraya + Mekong				656	1976-1990	10094	485	950	2.3	1.36
Xijiang	Wuzhou 3	23.48	111.3	330	1976-1983	7085	678	351	0.5	1.19
Changjiang	Datong	30.77	117.6	1705	1923-1986	25032	463	1649	0.5	1.20
Huanghe	Huayuankou	34.92	113.65	730	1946-1979	1465	63	789	1.4	2.61
Al Furat	Hindiya	32.72	44.27	274	1964-1972	678	78	355	4.4	5.07
Guadalquivir	Alcala del Rio	34.52	-5.98	47	1913-1984	434	291	69	0.6 (fit to runoff)	2.14
Loire	Montjean	47.38	-0.83	110	1863-1979	838	240	116	7.5	1.12
Odra	Gozdowice	52.77	14.32	110	1900-1987	536	154	129	1.7	1.36
N. Dvina	Ust-Pinega	64.10	42.17	348	1881-1985	3315	300	445	0.6	1.17
Volga*	Volgograd	48.40	44.5	1350	1879-1975	8137	190	1412	1.7	1.23
Don	Razdorskaya	47.50	40.7	378	1881-1984	787	66	481	no fit; with = 10, F_c = 1.30	1.91
Kura	Surra	40.12	48.67	178	1932-1984	547	97	95	2.4	1.33
Rhein	Rees	51.77	6.4	160	1936-1984	2291	453	154	0.5	1.03
Danube	Ceatal Izmail	45.18	28.8	807	1921-1984	6499	254	792	1.8	1.13
Wisla	Tczew	54.1	18.8	194	1900-1987	1055	171	227	1.9	1.24

* Probst and Tardy (1987), cited in Gleick (1993).

5.3.8.2 Regionalization

For the computation of water availability in the watersheds belonging to the above 43 river basins, the calibrated γ-values (and F_c values where necessary) are used. Each cell of a watershed gets the same parameter value. To the other watersheds (covering two thirds of the land surface of the earth), we assign parameter values using a simple regionalization algorithm that we have deduced from the calibration results. The regionalization parameters are the total available water capacity in the effective root zone S_{max}, the number of days below 0°C and the ratio of potential evapotranspiration over precipitation E_p/P averaged over the watershed. The regionalization proceeds as follows:

1. If $S_{max} > 150$ mm or the number of days per year below 0°C > 90, then γ is set to 0.7.
2. Otherwise, if $E_p/P > 2.8$, $\gamma = 10$ and the computed runoff R of each cell is divided by a correction factor F_c of 1.4
3. Otherwise, $\gamma = 2.0$

This scheme can only be expected to give a very rough indication of the correct value of γ. The scatter of the calibration data is obvious in Fig. 5.2, where the γ's of all calibration basins are drawn as a function of E_p/P, and those which fulfil condition 1 or condition 2 are designated. The parameter values assigned in the regionalization scheme correspond approximately to the mean parameter values of the three different groups of calibration basins.
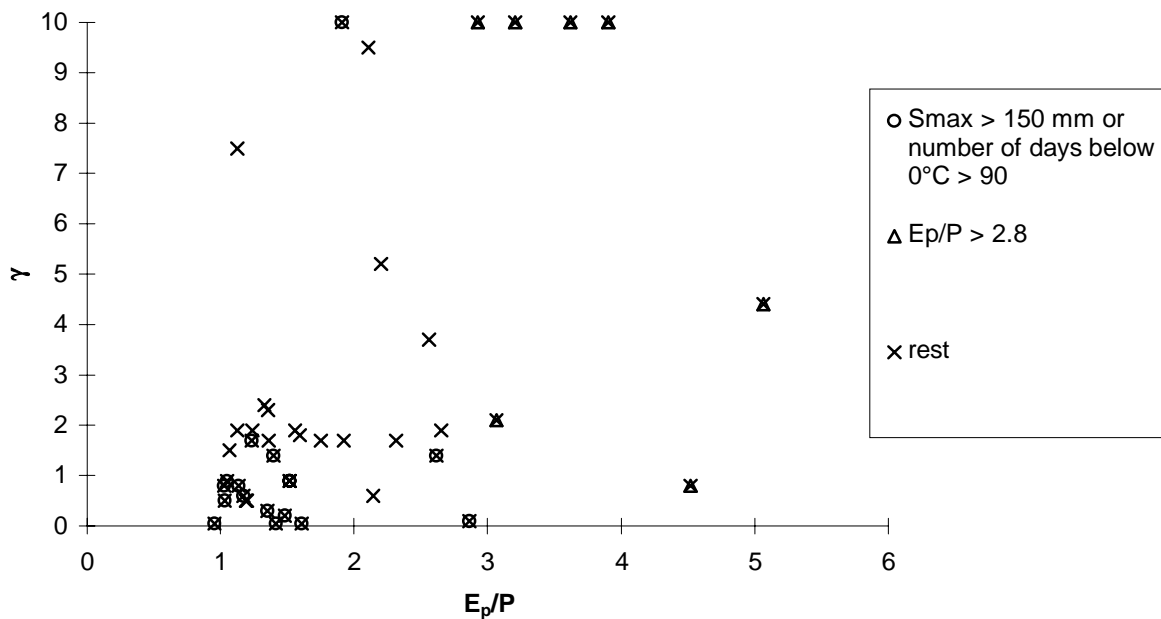

Fig. 5.2: Derivation of regionalization scheme from calibration to annual discharge in 43 river basins.

5.3.9 Comparison of WaterGAP estimates with other estimates

In Table 5.5, continental estimates of long-term average annual runoff computed by WaterGAP are compared with literature estimates. Generally, the WaterGAP estimates are rather low. For Asia, Europe & former USSR and North America, the WaterGAP estimate is the lowest of all five estimates.

A map of long-term average annual runoff computed by WaterGAP is given as Fig. A1 in the Appendix; it shows the runoff generated in each cell. The map is representative for the climatic conditions of the years 1931 to 1960. The overall spatial distribution of total long-term average runoff was compared to maps by the Institute of Geography, USSR Academy of Sciences, as depicted in WRI (1990, p. 169). The is a close correspondence between the two maps. However, WaterGAP 1.0 estimates lower total runoff values in Northern Algeria and Morocco as well as in Southeast China and Indochina.

Table 5.5: Comparison of WaterGAP 1.0 estimates of water availability in km^3/yr with literature estimates (based on summary table in Kulshreshtha, 1993, except for data from Baumgartner and Reichel, 1975).

Continent	WaterGAP 1.0 This paper[a]	L´vovich (1979)	Shiklomanov (1990)	World Resources Insitute (1990)	Baumgartner and Reichel (1975)
Asia (excl. Asian parts of former USSR)	8,974	9,865	9670	10,485	NA
Africa	4,057	4,225	4,570	4,184	3,397
Australia & New Zealand	1,142	731	348	2,011	2,394
Europe & former USSR	4,996	6,475	7,950	6,705	NA
Central America	603	545	NA	NA	NA
South America	10,471	10,380	11,760	10,377	11,062
North America	3,730	5,415	NA	NA	NA
North America & Central America	4,333	5,960	8,200	6,945	5,832

NA = Not available
[a] long-term average 1931-1960

5.4 Water use model

The various uses of water can be divided into uses for which water is withdrawn from its original location (withdrawal use) and uses of water in situ (instream use, such as shipping, hydroelectric power plants, habitat for aquatic life). Most water use data refer to withdrawal water use, which is divided into domestic, industrial and agricultural water use.

Part of the withdrawn water is returned to its source or to another location (return flow). The difference between withdrawal use and return flow is referred to as consumptive use, i.e. the amount of water which evaporates due to its withdrawal. Thus, a user might reuse the water that has already been withdrawn by a first user who returns (part of) it to the stream. If return

flow is high, like, for example, in the case of thermoelectric power plants (included in industrial water use), the amount of water used by two plants along a river in not much larger than that used by one. Then withdrawal use, which would be computed as the sum of the withdrawals for both plants, would overestimate the actual amount of water necessary to run the plants. On the other hand, consumptive use would underestimate it because for the first plant along the river, the amount equivalent to the withdrawal use of the first power plant must be available in the first place. Thus, actual water use lies between withdrawal and consumptive use. On a global scale, however, it is not possible to obtain this estimate. One would need to have information on

1. the quantity of return flows
2. quality of return flows and quality requirements of users
3. location of users within a watershed
4. instream uses

Available water use data mostly refer to withdrawal water use, except sometimes in the case of irrigation water use. The World Resources Institute (WRI) (1990, 1992, 1994, 1996) provides national withdrawal water use data of most countries of the globe, distinguishing domestic, industrial and agricultural water use. Altogether, national water use data for 160 countries are required. We directly use the national data of withdrawal use in the domestic and the industrial sector, and compute consumptive water use of these sector by multiplying withdrawal water use with an efficiency factor. We translate the national water use data, which are given as water use per person, to water use within a cell by taking into account population density, urbanization and access to safe drinking water (using different algorithms for domestic and industrial water use). In the case of agricultural water use, we use a different methodology. We subdivide agricultural water use into water use for livestock and water use for irrigation. Livestock water use is computed by multiplying livestock numbers with typical water use of one animal; it can be considered to be withdrawal water use. In the case of irrigation water use, however, we compute consumptive use from independent data on soil, climate and irrigated area using our hydrological model. We then relate the consumptive use to the national data of withdrawal use for agricultural purposes and determine an "irrigation correction factor" that reflects not only the irrigation efficiency but also the uncertainty of model and data. This procedure allows us to assess the influence of change of climate and irrigated area on irrigation water use.

5.4.1 Domestic water use

5.4.1.1 National data of withdrawal use

National data of domestic water use are taken from WRI (1990, 1992, 1994, 1996), except for 8 countries, for which we use values given by Niederländer and Dogterom (1996). The domestic water use is expressed as the domestic water use per person (per capita). From the available water use data, the value from the year closest to 1990 was selected. Depending on the country, the water use data are from the years 1965 to 1994 (most values being from the 80s and 90s). However, one must keep in mind that only the total water use is from the indicated years, while the division of total water use into the sectoral water uses (domestic, industrial and agricultural) was for most countries done for another year. For most countries outside Africa, this year was 1987 (WRI, 1996, p. 307). In order to reflect present-day water use, each national value is extrapolated to 1990 by using the same assumptions as made in Scenario M (see Section 3.3.1), and 1990 values of GDP (only if given year of maximum water use, in case of countries above a per cap GDP of US$ 15,0000, was before 1978, extrapolation to 1990 was done using scenario L if computations were to be made for Scenario L).

5.4.1.2 Allocation to grid cells

The domestic water use of people having easy access to drinking water is known to be higher than that of people without access. The World Bank (1996) and WRI (1996) provide national data on access to safe drinking water in urban and rural areas as well as the percentages of urban and rural population in each country. Access to safe drinking water in rural areas implies that a family member need not spend a "disproportionate" part of the day fetching water. In urban areas, access to safe drinking water is defined as access to piped water or a public standpipe within 200 m of a dwelling or housing unit.

We distribute the domestic water use of a country to the cells pertaining to it based on

- population density (data set "Global Population Density Map at 5 x 5 Minutes Resolution" of Tobler et al., 1995, as cited in van Woerden et al., 1995)
- percentage of rural and urban population in each country (WRI, 1996)
- percentages of inhabitants with access to safe drinking water in rural and urban areas (World Bank, 1996; WRI, 1996).

The steps for allocating national domestic water use values to cells are as follows:

1. Rural population density of a country is assumed to be the same in each of the country's cells. If the total population of a cell is less than the rural one, the difference is distributed equally within the country.
2. The difference between the total population of each cell and the rural population is assumed to be urban population.
3. The number of inhabitants in each cell that have access to safe drinking water is computed.
4. Those inhabitants without access to safe drinking water are assumed to have a domestic water use per capita of 3.65 m^3/yr (10 l/d). The rest of the national water use is equally distributed to each inhabitant with access to safe drinking water. If the national data for a country list a per capita domestic water use of less than 3.65 m^3/yr, the listed value is assumed to be valid for each inhabitant of this country.
5. The total domestic water use in a cell is computed as the sum of the water use by all the inhabitants without access to safe drinking water and those with access.

5.4.2 Industrial water use

5.4.2.1 National data of withdrawal use

National industrial water use data are taken from the same sources as the domestic water use data. Like the domestic water use, industrial water use is generally expressed as industrial water use per capita (WRI, 1996). Functionally, however, industrial water use rather depends on industrial production. Thus, for WaterGAP, per capita industrial water use is translated to industrial water use per industrial GDP. Industrial GDP is determined as a fraction of GDP, the fraction being given by the World Bank (1996) and WRI (1990, 1992, 1994, 1996), while GDP values of the years, for which water use data are available, are derived from UN (1995). As in the domestic sector, each national value for industrial water use is extrapolated to 1990 using the assumptions of scenario M (see Section 3.3.2) and 1990 values of GDP and Industrial GDP (only if given year of maximum water use, in case of countries above a per cap GDP of US$ 15,0000, was before 1978, extrapolation to 1990 was done using scenario L if computations were to be made for Scenario L).

5.4.2.2 Allocation to grid cells

Industry is assumed to exist only in urban areas. Thus, national industrial water use is allocated to grid cells according to their urban population. The total industrial water use of a country is equally distributed to all urban inhabitants (comp. section 3.1.2), and the industrial water use in a cell is the product of industrial water use per urban inhabitant and the number of urban inhabitants.

5.4.3 Agricultural water use

Agricultural water use can be roughly defined as the sum of water use for livestock and the water use for irrigation.

5.4.3.1 Livestock

Livestock water use is computed by multiplying the numbers of livestock in each cell by a livestock-specific water use. Table 5.6 lists the types of domestic animals and their specific water use. Data on the present density of livestock on a 1° by 1° resolution is provided by NCAR on the GlobalARC GIS Database (1996) except for chicken. Chicken population density is derived from country-specific data (WRI, 1996); the chicken were then equally distributed over the cells of each country. Total livestock water use in a cell is computed by multiplying livestock-specific water use per animal (UN, 1986; cited in Kulshreshtha, 1993) with the numbers of the specific livestock, and then summing over all the livestock types. The UN livestock-specific water use values are low compared to water requirements given in many books on animal production (e.g. 5 l/d might be typical for sheep, and 50 l/d for cattle according to Jeroch, 1986).

Table 5.6: Livestock-specific water use.

livestock	water use [l/d per animal]
cattle	25
pigs	4
sheep	2.25
goats	2.25
chicken	0.028
horses	15
camels	25
buffalo	25

5.4.3.2 Irrigation

Only part of the water withdrawn for irrigation is actually used up by the crop. This part is called consumptive use. The rest is either "lost" by evaporation or seepage between the withdrawal point and the application point or is necessary to leach the salts in the soil. The ratio of consumptive use and withdrawal use is called irrigation efficiency. Once the location and extent of irrigated areas is known, consumptive use can be determined as a function of climate, crop, cropping intensity and soil type. In WaterGAP, the dependence on crop and soil type is neglected mainly because it is not known which crop grows where.

5.4.3.2.1 Irrigated area

The FAO supplies data of total irrigated area for each country; there do not, however, exist continental-scale maps of irrigated areas except for Africa. Therefore, we use an algorithm of Klepper (1996) that distributes the total irrigated area (1990 values from FAO) within each

country. 1/12° by 1/12° grid cells are assigned to be either irrigated or not irrigated based on the following scheme.

1. Irrigation only occurs if grid cell is less than 50 km away from a river.
2. The grid cells of each country which fulfill this requirement are ranked according to a weight computed as

$$
W(1/12° \text{ cell}) = \quad W_{suitability} * [\text{soil suitability}] +
$$
$$
W_{landcover} * [\text{land cover irrigation likelyhood class}] +
$$
$$
W_{population} * [\text{population density}]
$$

3. Within each country, the cells with the highest weights are consecutively assigned to be irrigated until the total irrigated area of the country is allocated.
4. The resulting global binary map at 1/12° resolution is then transformed to a map at 0.5° resolution, where the fraction of land that is irrigated is represented.

Soil suitability is computed based on the FAO Soil Map of the World and a slightly modified table of soil specific reduction factors listed by Leemans and van den Born (1994) which takes into account fertility, salinity, acidity, drainage and rooting depth. Soil suitability ranges from 0 (not suitable) to 100 (very suitable). Land cover irrigation likelihood class is based on the landcover map of Olson et al. (1985), the resolution of which is too coarse (1/6°, but mostly 1/2°) to be directly applicable. Klepper thought that seven of the 58 land cover types of Olson et al. may indicate that irrigation occurs, and assigned them to three land cover irrigation likelihood class (Table 5.7). Population density is expressed in inhabitants per km^2; the data set "Global Population Density Map at 5 x 5 Minutes Resolution" of Tobler et al. (1995, as cited in van Woerden et al. (1995) is used. Klepper found that the irrigation map of Africa could best be simulated by setting $W_{suitability}$ to 0.1, $W_{landcover}$ to 25 and $W_{population}$ to 1. Obviously, population density is a strong "predictor" of irrigation, while soil suitability is only a weak one.

Table 5.7: Conversion table between the land cover types of Olson et al. (1985) and land cover irrigation likelihood class (from Klepper, 1996).

land cover irrigation likelihood class	Olson et al. land cover
1 (may contain some irrigated land if other factors are highly favorable)	CFS (cool farmland and settlements, more or less snowy) MFS (mild/hot farmland and settlements) FWG (field/woods with grass and/or cropland)
2 (may contain irrigated land)	CCI (cool cropland with irrigation of variable extent) CCP (cold cropland and pasture, irrigated locally)
3 (may include considerable portion of irrigated land)	PRA (paddy rice and associated Land Mosaics) WCI (warm/hot cropland, irrigated extensively)

5.4.3.2.2 Consumptive use

The consumptive use of irrigation is equal to the additional amount of evapotranspiration that occurs due to irrigation. It is the fraction of actually applied irrigation amount which evapotranspirates. The consumptive use depends on climate as well as on crop, cropping

intensity and soil type. In this assessment, the dependence on crop and soil type is neglected mainly because it is not known which crop grows where. Consumptive use in each irrigated cell is computed by

1. determining the days on which irrigation is necessary based on conditions for "natural" growing and the required length of the growing period
2. computing the (net) irrigation amount on the irrigation days such that the sum of precipitation and irrigation (consumptive use) is equal to potential evapotranspiration
3. multiplying the thus computed consumptive use with the fraction of irrigated area within the cell.

According to FAO (1981), a normal natural growing season is characterized by precipitation P_{eff} being larger than potential evapotranspiration E_p and temperature T being higher than 5°C. The thus computed natural growing season is increased by the time it takes for the crop to empty the soil moisture supply. Based on this concept, we devised a simple algorithm to compute the irrigation period.

The period required for crop growth is set to a standard value of 150 d. This growing period corresponds to a cropping intensity of 1. If cropping intensity is smaller than 1, not the whole irrigated area is cropped every year. If cropping intensity is larger than 1, more than a single crop is grown. Cropping intensities on irrigated areas for 13 world regions are given in Table 5.8. The 13 world regions are those used in IMAGE (Alcamo et al., 1994a). The values for developing countries are specific for irrigated areas in the period of 1988-1990 and are taken from Alexandratos (1995), while the other values are from an estimate of Klepper (1996). In order to account for cropping intensities smaller than 1, the consumptive use of each irrigated cell is multiplied with the cropping intensity. In order to account for cropping intensities larger than 1, a fraction of the cells of a world region is assumed to require a growing period of 300 d instead of 150 d. With a cropping intensity of, for example, 1.2, the consumptive use of 20 percent of a region's irrigated area is computed with a growing period of 300 d. Those cells within a world region are favored which due to their temperature regime allow a 300 d growing period and require the least irrigation days (see next two paragraphs). A day is defined to be a "natural" growing day if

1. $T > 5°C$
2. $P_{eff} > E_p$ ($P_{eff} > 0.5 E_p$ in first 30 days of the growing season)
3. $S > 0$ mm
4. $P_{eff} > 0.01$ mm/d

As expressed in condition 2, during the first month of the growing season it is sufficient for precipitation to be half the potential precipitation, while later precipitation should be larger than potential evapotranspiration. This requirement roughly takes account of the fact that during the early growing stage the plants are still small and thus transpire much less water than later in the growing season. It is consistent with the mean behavior of a variety of crops if we assume that reference crop evapotranspiration is equal to potential evapotranspiration (comp. the crop factors and duration of growth stages by Brouwer and Heibloem, 1986).

If, on a given day, condition 1 is fulfilled, but conditions 2 to 4 are not, irrigation is necessary for crop growth. For each irrigation day, consumptive use is computed as $E_p - P_{eff}$ (for the first 30 days: $0.5 E_p - P_{eff}$). The cell-specific consumptive use is obtained by multiplication with the fraction of irrigated area within the cell. The cell-specific growing period is computed by finding the period of 150 days length during which the number of irrigation days is smallest. The procedure to find the 300 d growing period is the same. In the case of a few irrigated cells, it happens that no period of 150 d can be found with T > 5°C. Then, the growing period continues into the time period with T ≤ 5°C. If not enough cells with 300 days greater or equal 5°C can be found within a region, consumptive use is first computed with the possible

number of cells with 300 d growing period; the consumptive use is then corrected by multiplication with the ratio of the regional cropping intensity of Table 5.8 and the (lower) cropping intensity implemented in the model. If in very arid regions P_{eff} is never larger than 0.5 E_p, January 1st is assumed to be the start of the irrigation period.

The above described method to compute consumptive water use can result in an underestimation of actual consumptive use because

- actual use is prone to be larger than the modelled optimal use
- interannual variability leads to irrigation use in low precipitation years, while the surplus water of high precipitation years cannot be transferred to low precipitation years
- daily precipitation variability may lead to irrigation use (we only use mean monthly precipitation values)

Table 5.8: Regional cropping intensities and water use efficiencies.

IMAGE region	cropping intensity 1995[a]	cropping intensity 2025 and 2075[b]	irrigation water use efficiency (estimated from project efficiencies)[c]	computed irrigation correction factor
Canada	1.0	1.0	0.45	0.42
USA	1.0	1.0	0.30	0.17
Latin America	0.9	1.0	0.26	0.30
Africa	0.9	1.0	0.41	0.29
OECD Europe	1.0	1.0	0.35	0.48
Eastern Europe	1.0	1.0	n.a.	0.52
former USSR	0.8	0.8	n.a.	0.36
Middle East	1.0	1.1	0.31	0.96
India and South Asia	1.2	1.4	0.20	0.39
China and centrally planned countries	1.5	1.5	n.a.	0.51
East Asia	1.2	1.3	0.33	0.05
Oceania	1.5	1.5	n.a.	0.89
Japan	1.5	1.5	0.22	0.03

[a] from 1988/90 data in Alexandratos (1996) for developing countries excl. China and Klepper (1996) for others
[b] from 2010 data in Alexandratos (1996) for developing countries excl. China; no change with respect to 1995 for others
[c] Bos and Nugteren (1982)
n.a.: data not available

5.4.3.2.3 Withdrawal use

Estimates of irrigation efficiency of 50 irrigation projects in various countries were obtained by Bos and Nugteren (1982) by sending out questionnaires to irrigation project officer (Table 5.8). On the other hand, there exists data on agricultural withdrawal water use for (almost) each country (WRI, 1996; Niederländer and Dogterom, 1996). We subtract livestock water use as computed by WaterGAP from these values and obtain "literature values of irrigation withdrawal use". Then, for each country, we determine the so-called irrigation correction factor as the ratio of consumptive use (computed by WaterGAP with the 1995 average precipitation) and the "literature value". If model and data were correct, the computed irrigation correction factor should be similar to the irrigation efficiencies of Bos and Nugteren. However, the correction factor also includes, on the model side, the errors due to the allocation of irrigated area within a country, due to the algorithm to compute consumptive use per irrigated area and due to the

selection of the cropping intensity. On the data side, the errors in the total irrigated area per country and in the agricultural water use per country are reflected. All the errors might be considerable. Therefore, the correction factor varies widely, ranging from $1 \cdot 10^{-6}$ to 9, the majority ranging between 0.001 and 1. The mean irrigation correction factors of each region are listed in Table 5.8. Note that the coefficient of variance is typically around 1.

For the computation of irrigation withdrawal use, we have decided to trust more the country data on agricultural water use than our model. Therefore, we divide the consumptive use computed by WaterGAP by the (national) irrigation corrections factors. Keeping these correction factors constant for each year and also when applying the 1-in-10-years precipitation instead of the average precipitation, our model can compute the influence on irrigation water use of the following factors:

- climate change due to greenhouse gases
- increase of irrigated agricultural area and cropping intensity
- increased water use in dry years

Any possible increase in water use efficiency can be expressed by an increase of the correction factor.

However, if the irrigation correction factor is less than, let us say, 0.1, it might well be that the model underestimates consumptive use for average precipitation in 1995 considerable. If such a low correction factor is used for low flow conditions, the withdrawal use for a 10-percentile dry year might well be overestimated.

The algorithm to compute the distribution of irrigated area still uses the former USSR and CSSR as single entities, instead of the new countries. Now that data of irrigated areas for each of the new countries exist, it is obvious that the algorithm to allocate irrigated areas does not function well in these areas. The best solution at the moment is to still compute the effect of climate change, water use efficiency increase and 1-in-10-years precipitation with the consumptive use model, then to average the effect over all the countries of the former USSR and CSSR, respectively, and finally to scale the literature values of irrigation withdrawal use with the computed factors.

A particular problem is that there are some countries for which our model does not compute any consumptive use for average precipitation of 1995 although there exists an appreciable irrigated area of more than 500 km^2 (Costa Rica, El Salvador, Guatemala, Guyana, Suriname, Uruguay, Lebanon, The Philippines, Swaziland). Some of the reasons for this are given in Section 5.7.2.2. For many of these countries, a consumptive use is computed for 1-in-10 dry years (or increased irrigated area in the future). For these countries, we cannot, however, determine an irrigation correction factor; Therefore, in all countries, where a consumptive use of zero is computed in the case of 1995 average precipitation, we just take the "literature values of irrigation withdrawal use" as the irrigation withdrawal use under average precipitation. In case of the three countries with irrigation correction factors of less than 0.001, we do the same. For these countries, we cannot model the increased irrigation water use in a 10-percentile dry year, nor the impact of climate change on irrigation water use. The effect of increased water use efficiency and increase in irrigated area, however, can be taken into account by simple scaling.

6. Freshwater criticality ratio

A freshwater criticality index can be based on the ratio of water need over available water resources. Here, however, only water use instead of water need could be computed. Thus, areas were water use is already restricted by (natural) water availability (but also lack of infrastructure etc.) might not appear to be critical. To be on the safe side, one should look at withdrawal water use because

1. instream uses are not considered here
2. the quality of return flow is unknown
3. the location of the water users within the watershed is not known

The available water resources are defined as the amount of water that is sustainably available. It is the runoff (as surface runoff and groundwater recharge) produced within the spatial entity of interest during a given time period under the indicated climatic conditions. Very important for the estimation of water availability but also of water use is the spatial and temporal scale. For this report, we compute the internally renewable water resources of whole watersheds throughout a year. We do not consider the water flowing into or out of the watershed, which might over- or underestimate the amount of water that is actually available within a watershed. However, it is appropriate to just look at the internally renewable resources, because imported water should be considered to be a resource that does not "belong" to the watershed but that is just a (temporary?) "loan" from the upstream watershed. Looking at whole watersheds neglects the differences in water available upstream and downstream. Looking at annual values results in underestimating the criticality during months of high irrigation water demand and low precipitation if water supply is from surface water. At this stage of our research, we cannot, however, look at monthly values because we have not calibrated our hydrological model to measured monthly discharge values.

Here, we call the ratio of annual water use within a watershed over the annual runoff produced within a watershed the freshwater criticality ratio. This definition implies the assumption that withdrawn water can be transported within the watershed without restrictions; it is consistent with

- the fact that generally water cannot be transported across watershed boundaries but relatively easy within a watershed, and
- the idea that water supply and use should be managed on the watershed scale (i.e., for example, not within country boundaries in case of an international watershed).

Such a criticality ratio should not be computed for average annual conditions of water availability and use only, but also for more critical conditions representative of years that are drier than normal. Here, we determine both a criticality index for average precipitation conditions ($C_{average}$) and one for 10-percentile dry conditions (C_{10d}). For the latter index, we compute the water available and used during a 10-percentile dry year (i.e. only 1 in 10 years has less precipitation than such a 10-percentile dry year). While the amount of surface water available is computed with the 10-percentile precipitation, we assume that the amount of groundwater which is sustainably available in this year is that of the average year. The amount of irrigation water required is also particular for the 10-percentile precipitation, while domestic and industrial water use do not vary with precipitation. The freshwater criticality ratios of watersheds are defined as

$$C_{average} = \frac{\overset{watershed}{\sum} annual\ withdrawal\ water\ use\ in\ cell\ during\ average\ year}{\overset{watershed}{\sum} annual\ runoff\ in\ cell\ during\ average\ year} \qquad (13)$$

$$C_{10d} = \frac{\overset{watershed}{\sum} annual\ withdrawal\ water\ use\ in\ cell\ during\ 10-percentile\ dry\ year}{\overset{watershed}{\sum} annual\ runoff\ in\ cell\ during\ 10-percentile\ dry\ year} \qquad (14)$$

Following Kulshreshtha (1993), we combine the freshwater criticality ratio with the water availability per capita to obtain a freshwater criticality index. This index ranges between 1 for water surplus to 4 for water scarcity. Given the same criticality ratio, the watershed is more vulnerable with respect to water resources if the per capita water availability is low. For example, if water use is restricted by (low) water availability, the criticality ratio may be relatively low, but the situation should be called critical. Table 6.1 shows the definition of the freshwater criticality index; it is defined on the watershed scale.

The criticality ratio and the criticality index of countries computed exactly like that of watersheds. This method does not reflect correctly the influence of international watersheds on the water availability of a country. However, as we do not currently take into account the topology within and between watersheds, this approach is appropriate.

Table 6.1: Definition of the freshwater criticality index (after Kulshreshtha, 1993).

per capita water availability [m^3/(cap yr)]	criticality ratio (use/availability)			
	< 0.4	0.4 - 0.6	0.6 - 0.8	> 0.8
< 2,000	2	3	4	4
2,000-10,000	1	2	3	4
> 10,000	1	1	2	4

1: water surplus
2: marginally vulnerable
3: water stress
4. water scarcity

References

Alcamo, J., Kreileman, G.J.J., Bollen, J.C., van den Born, G.J., Gerlagh, R., Krol, M.S., Toet, A.M.C., de Vries, H.J.M. (1996): Baseline scenarios of global environmental change. Global Environmental Change, 6, 261-304.

Alcamo, J., Kreileman, G.J.J., Krol, M.S., Zuidema, G. (1994a) Modeling the global society-biosphere-climate system: Part 1: Model description and testing. Water, Air and Soil Pollution 76, 1-35.

Alcamo, J., van den Born, G.J.J., Bouwman, A.F., de Haan, B.J., Klein Goldewijk, K., Klepper, O., Krabec, J., Leemans, R., Olivier, J.G.J., Toet, A.M.C., de Vries, H.J.M, van der Woerd, H.J. (1994b): Modeling the global society-biosphere-climate system: Part 2: Computed scenarios. Water, Air and Soil Pollution 76, 37-78.

Alexandratos, N. (ed.) (1995): World Agriculture: Towards 2010 - An FAO Study. John Wiley & Sons, Chichester.

Batjes, N.H. (1996): Development of a world data set of soil water retention properties using pedotransfer rules. Geoderma 71, 31-52.

Baumgartner, A., Reichel, E. (1975): Die Weltwasserbilanz. R. Oldenbourg.

Bederke, E., Wunderlich, H.G. (1968): Großer physikalischer Weltatlas. II. Geologie. Meyers Verlag.

Bergström, S. (1994): The HBV model. In Singh, V.P. (ed.): Computer Models of Watershed Hydrology. Water Resources Publications 443-476.

Bergström, S. (1990): Parametervärden för HBV-modellen i Sverige. SMHI Hydrologi no. 28.

Bos, M.G., Nugteren, J. (1978): On Irrigation Efficiencies. International Institute for Land Reclamation and Improvement.

Dierke (1975): Atlas.

FAO (1991): FAO Soil Map of the World. World Soil Resources Report 67 (Release 1.0). FAO, Rome.

FAO (1981): Report on the agro-ecological zones project. Vol. 3 Methodology and results for South and Central America. FAO, Rome.

Forsythe, W.C., Rykiel Jr., E.J., Stahl, R.S., Wu, H., Schoolfield, R.M. (1975): A model comparison for daylength as a function of latitude and day of year. Ecol. Modelling 80, 87-95.

Gleick, P.H. (1993): Water in Crisis: A Guide to the World's Fresh Water Resources. Oxford University Press, New York.

GlobalARC GIS Database (1996) by CRSSA, Rutgers University and U.S. Army CERL.

Grabs, W., De Couet, T., Pauler, J. (1996): Freshwater fluxes from continents into the world oceans based on data of the Global Runoff Data Base. Report no. 10, Global Runoff Data Centre, Federal Institute of Hydrology, Koblenz, Germany.

Hutchinson, M.F. (1995): Interpolating mean rainfall using thin plate smoothing splines. Int. J. Geogr. Inf. Syst. 9, 385-403.

IAH (1974-1990): International Hydrogeological Map of Europe 1:1 500 000. Various sheets. Bundesanstalt für Geowissenschaften und Rohstoffe, Hannover, Germany - UNESCO Paris.

Intergovernmental Panel on Climate Change: J.T. Houghton, B.A. Callendar, S.K. Varney (eds.) (1992): Climate Change 1992. The Supplementary Report to the IPCC Scientific Assessment. Cambridge University Press.

Jarvis, P.G. (1976): The interpretation of the variations in leaf water potential nd stomatal conductance found in canopies in the field. Phil. Trans. R. Soc. B237, 593-610.

Jeroch, H. (1986): Vademekum der Fütterung. VEB Gustav Fischer Verlag Jena.

Klepper, O. (1996): Documentation for the calculation of world-wide water satisfaction on catchment basin level. Unpublished report, RIVM, The Netherlands.

Kulshreshtha, S.N. (1997): Personal communication.

Kulshreshtha, S.N. (1993): World Water Resources and Regional Vulnerability: Impact of Future Changes. RR-93-10, IIASA , Laxenburg, Austria.

Leemans, R., van den Born, G.J (1994): Determining the potential distribution of vegetation, crops and agricultural productivity. Water, Air and Soil Pollution 76, 133-161.

Leggett, J., W.J. Pepper and R.J. Swart. 1992: Emission Scenarios for the IPCC: An Update. In: IPCC, Climate Change 1992: The Supplementary Report to the IPCC Scientific Assessment. Cambridge University Press, Cambridge.

Lozar, R. (1992): Global climatic change management by watershed basin units. Proceedings of the American Society of Photogrametry and Remote Sensing, August 92, ASPRS, Bethesda MD, Volume 4, 150-.

Manabe, S., Spelman, M.J., Stouffer, R.J. (1992): Transient response of a coupled ocean-atmosphere model to gradual changes of atmospheric CO_2. Part 2: Seasonal response. J. Climate 5, 105-126.

Manabe, S., Stouffer, R.J., Spelman, M.J., Bryan, K. (1991): Transient response of a coupled ocean-atmosphere model to gradual changes of atmospheric CO_2. Part 1: Annual mean response. J. Climate 4, 785-818.

Marks, D., Dozier, J. (1992): Climate and energy exchange at the snow surface in the alpine region of the Sierra Nevada, 2. Snow cover energy balance. Water Resour. Res. 28, 3043-3054.

Mays, L.W. (1996): Water Resources Handbook. McGraw-Hill.

McNaughton, K.G., Jarvis, P.G. (1991): Effects of spatial scale on stomatal control of transpiration. Agric. For. Meteorol. 62, 279-302.

Niederländer, H.A.G., Dogterom, J. (1996): Water demand as supply and water related emissions in the domestic, agricultural and industrial sectors - An inventory of world-wide data coverage. ICWS Report 96.03.

Olson, J., Watts, J.A., Allison, L.J. (1985): Major world ecosystem complexes ranked by carbon in live vegetation: A database. Report NDP-017, Oak Ridge National Laboratory, Oak Ridge, Tennessee 164 pp.

Priestley, C., Taylor, R. (1972): On the assessment of surface heat flux and evaporation using large scale parameters. Mon. Weather Rev. 100, 81-92.

Riehl, H. (1979): Climate and Weather in the Tropics. Academic Press.

Röckner, E., Arpe, K., Bengtsson, L., Christoph, M., Claussen, M., Dümenil, L., Esch, M., Giorgetta, M., Schlese, U., Schulzweida, U. (1996): The atmospheric general circulation model ECHAM-4: Model description and simulation of present day climate. MPI-Report No. 218, MPI für Meteorologie, Hamburg.

Shuttleworth, W.J. (1993): Evaporation. In Maidment, D.R. (ed.): Handbook of Hydrology. McGrawHill 4.1-4.53.

UN Department for Economic and Social Information and Policy Analysis Statistical Division (1995): Statistical Yearbook 1993. UN, New York.

UN (1988): Africa: Major Hydrogeological Formations. After Geological Map of Africa 1:5 000 000. Map no. 2033, revision 1. UN, New York.

UN (1987): Fertility Behavior in the Context of Development. Population Studies 100.ST/ESA/SER.A/100. Dept of International Economic and Social Affairs: New York.

van Woerden, J. W., Diederiks, J., Goldewijk, K.Klein (1995): Data Management in Support of Integrated Environmental Assessment and Modelling at RIVM - Including the 1995 RIVM Catalogue of International Data Sets . RIVM Report No. 402001006.

World Bank (1991): World Development Report 1991. Oxford University Press, New York.

World Bank (1996): World Development Report 1996. Oxford University Press.

World Resources Institute (1996): World Resources (1996-97) - A Guide to the Global Environment: The Urban Environment. Oxford University Press